Cosmic axion thermalization

O. Erken, P. Sikivie, H. Tam, and Q. Yang

Phys. Rev. D **85**, 063520 — Published 28 March 2012

DOI: 10.1103/PhysRevD.85.063520

Cosmic axion thermalization

O. Erken, P. Sikivie, H. Tam and Q. Yang[1]

[1]*Department of Physics, University of Florida, Gainesville, FL 32611, USA*

(Dated: February 1, 2012)

Axions differ from the other cold dark matter candidates in that they form a degenerate Bose gas. It is shown that their huge quantum degeneracy and large correlation length cause cold dark matter axions to thermalize through gravitational self-interactions when the photon temperature reaches approximately 500 eV. When they thermalize, the axions form a Bose-Einstein condensate. Their thermalization occurs in a regime, herein called the 'condensed regime', where the Boltzmann equation is not valid because the energy dispersion of the particles is smaller than their interaction rate. We derive analytical expressions for the thermalization rate of particles in the condensed regime, and check the validity of these expressions by numerical simulation of a toy model. We revisit axion cosmology in light of axion Bose-Einstein condensation. It is shown that axions are indistinguishable from ordinary cold dark matter on all scales of observational interest, except when they thermalize or rethermalize. The rethermalization of axions that are about to fall in a galactic potential well causes them to acquire net overall rotation as they go to the lowest energy state consistent with the total angular momentum they acquired by tidal torquing. This phenomenon explains the occurrence of caustic rings of dark matter in galactic halos. We find that photons may reach thermal contact with axions and investigate the implications of this possibility for the measurements of cosmological parameters.

PACS numbers: 95.35.+d

I. INTRODUCTION

One of the outstanding problems in science today is the identity of the dark matter of the universe [1]. The existence of dark matter is implied by a large number of observations, including the dynamics of galaxy clusters, the rotation curves of individual galaxies, the abundances of light elements, gravitational lensing, and the anisotropies of the cosmic microwave background radiation. The energy density fraction of the universe in dark matter is observed to be 23%. The dark matter must be non-baryonic, cold and collisionless. *Non-baryonic* means that the dark matter is not made of ordinary atoms and molecules. *Cold* means that the primordial velocity dispersion of the dark matter particles is sufficiently small, less than about 10^{-8} c today, so that it may be set equal to zero as far as the formation of large scale structure and galactic halos is concerned. *Collisionless* means that the dark matter particles have, in first approximation, only gravitational interactions. Particles with the required properties are referred to as 'cold dark matter' (CDM). The leading CDM candidates are weakly interacting massive particles (WIMPs) with mass in the 100 GeV range, axions with mass in the 10^{-5} eV range, and sterile neutrinos with mass in the keV range. To try and tell these candidates apart on the basis of observation is a tantalizing quest.

For a long time, it was thought that axions and the other forms of cold dark matter behave in the same way on astronomical scales and are therefore indistinguishable by observation, whether it be observations of large scale structure or measurements of cosmological parameters. More recently, however, it was pointed out that dark matter axions form a Bose-Einstein condensate (BEC), as a result of their gravitational self-interactions, when the photon temperature reaches about 500 eV [2]. Axions or axion-like particles are special because they are a degenerate Bose gas. The other dark matter candidates, which we refer to henceforth as 'ordinary cold dark matter', are non-degenerate. This raises the question whether axions may be observably different after all. It was shown in Ref. [2] that, on all scales of observational interest, density perturbations in axion BEC behave in exactly the same way as those in ordinary cold dark matter provided the density perturbations are within the horizon and in the linear regime. On the other hand, when density perturbations enter the horizon, or in second order of perturbation theory, axions generally behave differently from ordinary cold dark matter because the axions rethermalize to let the axion state (i.e. the state most axions are in) track the lowest energy state [2].

Axion Bose-Einstein condensation appears to resolve a puzzle that has arisen in the study of the inner caustics of galactic halos. The structure of the inner caustics depends on the angular momentum distribution of the infalling particles. If the particles fall in with net overall rotation, the inner caustics are rings whose cross-section is a section of the elliptic umbilic (D_{-4}) catastrophe, called 'caustic rings' for short [3, 4]. If the velocity field of the infalling particles is irrotational, the inner caustics have a 'tent-like' structure which is described in detail in Ref. [5] and which is quite distinct from that of caustic rings. The radii of the caustic rings, assuming that the dark matter falls in with net overall rotation, were predicted [3] using the self-similar infall model of galactic halos [6], generalized to allow angular momentum for the infalling particles [7, 8]. Evidence was found for the existence of caustic rings at the predicted

radii. The evidence is summarized in Ref. [8]. Now, the puzzle is that ordinary cold dark matter has an irrotational velocity field [5] and is therefore incompatible with the existence of caustic rings. Axion Bose-Einstein condensation resolves the puzzle provided the axions rethermalize sufficiently quickly that most of them go to the lowest energy available state before falling in [2, 9]. The lowest energy state consistent with the total angular momentum the axions will have acquired from neighboring inhomogeneities by tidal torquing is a state of rigid rotation on the turnaround sphere, the simplest form of net overall rotation. Therefore, if the dark matter is an axion BEC that rethermalizes sufficiently quickly, the inner caustics are rings. Furthermore it was shown [9] that the caustic rings are all in the same plane (that of the galactic disk), that the overall size of the rings is predicted correctly by tidal torque theory, and that the relative sizes of the rings are precisely as predicted by the self-similar model and therefore consistent with the evidence for caustic rings published earlier. One thing remains to be done: to show that axions about to fall into a galactic potential well rethermalize sufficiently quickly that they almost all go to the lowest energy available state. It is one of the goals of this paper to understand cosmic axion thermalization sufficiently well to be able to verify this.

The existence of caustic rings in dark matter halos has been challenged on the basis of numerical simulations of galaxy formation [10]. However, present simulations have inadequate resolution to see but a few of the expected caustics [11]. Moreover, the simulations do not include the physics of axion Bose Einstein condensation which is an essential ingredient in the formation of the rings.

There is a second motivation for studying the thermalization rates of dark matter axions in detail [12]. We mentioned that cold axions thermalize by their gravitational interactions. But gravity is universal. If axions thermalize by gravitational interactions, they may also enter into thermal contact with other species. If the axions enter into thermal contact with the cosmic photons, the photons will cool and some cosmological parameters, in particular the baryon to photon ratio at primordial nucleosynthesis and the effective number of neutrinos (a measure of the radiation density at the time of decoupling), will be modified compared to their values in the standard cosmological model. This opens the possibility of being able to distinguish axions from the other forms of cold dark matter by measuring cosmological parameters.

Due to their unusual properties, dark matter axions occupy a unique and uncharted region in the physics of many-body systems. On the one hand, they are highly condensed, which greatly exaggerates the quantum effect of Bose-enhancement in scattering processes. On the other, the fact that their energy dispersion is very small implies that they are outside the realm of the 'particle kinetic regime'. In this case, the picture of instantaneous collisions breaks down, so that the usual Boltzmann equation no longer applies. Together, these properties – high occupation number and small energy dispersion – are highly atypical, and thus very little attention has been paid to the study of such systems. Existing techniques in non-equilibrium statistical mechanics are not applicable to dark matter axions, rendering the estimation of their thermalization rate non-trivial.

The outline of this paper is as follows. In Section II, we give a definition of cold dark matter and ask under what conditions axions behave as such. We find that axions behave as CDM on all scales of observational interest except when they thermalize or rethermalize. In Section III, we derive expressions for the thermalization rate of particles in the 'condensed regime', i.e. when their energy dispersion is small compared to their interaction rate. The condensed regime is the one relevant to cosmic axion thermalization. In Section IV, we check the validity of our estimates of thermalization rates in the condensed regime by numerical simulation of a toy model. In Section V, we revisit axion cosmology in light of axion thermalization and Bose-Einstein condensation. Section VI provides a summary.

II. AXIONS ARE DIFFERENT

Both axions and WIMPs are considered forms of cold dark matter. Furthermore, until recently, axions and WIMPs were thought to be indistinguishable on observational grounds, i.e. indistinguishable on the basis of purely astronomical data. The discovery [2] that dark matter axions form a Bose-Einstein condensate has changed this view since axion BEC is claimed to have observable consequences [2, 9, 12]. This raises questions. First, precisely under what conditions are axions and WIMPs cold dark matter? Second, if both axions and WIMPs are CDM, how do they differ? There is a preliminary question: how is cold dark matter defined?

The purpose of this section is to discuss these three questions in a general way, to set the stage for the more detailed calculations that follow. For the sake of brevity, we call WIMPs all cold dark matter candidates which do not form a degenerate Bose gas. As far as we are aware, this includes all cold dark matter candidates except axions and axion-like particles. In particular, *sterile* neutrinos are called WIMPs here. (Neutrinos are not WIMPs since they are hot dark matter.)

To start off it is worth emphasizing that, at the fundamental level, axions and WIMPs are very different. The surprise is really that they have similar properties as far as large scale structure is concerned. Both axions and WIMPs are described by quantum fields. Furthermore, both are excellently described by classical limits of quantum

fields. But the classical limits are different in the two cases: WIMPs are in the classical particle limit whereas (decoupled) axions are in the classical field limit. In the classical particle limit one takes $\hbar \to 0$ while keeping $E = \hbar\omega$ and $\vec{p} = \hbar\vec{k}$ fixed. Since $\omega, \vec{k} \to \infty$, the wave nature of the quanta disappears. WIMPs are to excellent approximation classical point particles. In the classical field limit, on the other hand, one takes $\hbar \to 0$ for constant ω and $\vec{k}$. $E = \mathcal{N}\hbar\omega$ and $\vec{p} = \mathcal{N}\hbar\vec{k}$ are held fixed by letting the quantum state occupation number $\mathcal{N} \to \infty$. This is the limit in which quantum electrodynamics becomes classical electrodynamics. It is the appropriate limit for (decoupled) cold dark matter axions because they are a highly degenerate Bose gas. The axion states that are occupied have huge occupation numbers, $\mathcal{N} \sim 10^{61}$ [2]. The need to restrict to *decoupled* axions will be explained shortly.

So axions and WIMPs are fundamentally different even if it turns out that both can legitimately be called CDM. The distinction is not just academic, and is certainly important if axions thermalize, i.e. if axions find a state of larger entropy through self-interactions. Recall that, whereas statistical mechanics makes sense of the behaviour of large aggregates of classical particles (it was invented by Boltzmann to derive the properties of atoms in the gaseous state) it fails to make sense of classical fields. In thermal equilibrium every mode of a classical field would have average energy $k_{\rm B}T$. As Rayleigh pointed out, the energy density is infinite then at finite temperature due to the contributions from short wavelength modes. Thus the application of statistical mechanics to classical field theory (classical electrodynamics in particular) is in direct disagreement with observation. As is well-known, the disagreement is removed because of, and only because of, quantum mechanics.

What do we learn from this? If the axions are decoupled (i.e. do not interact and hence do not thermalize), they behave to excellent approximation like classical fields. As such, they are quite different from WIMPs since WIMPs are classical particles. So the argument why decoupled axions behave as CDM must be different from the argument why WIMPs behave as CDM. If the axions thermalize, they are not even described by classical fields. Instead they form a Bose-Einstein condensate, an essentially quantum-mechanical phenomenon. If the axions form a BEC, the argument why the axion BEC behaves as CDM must be different again.

The main purpose of this paper is, in fact, to show that axions thermalize as a result of their gravitational interactions, that they form a BEC, and that a rethermalizing axion BEC behaves differently from CDM. This will be done in Sections III, IV and V. In the remainder of the present section, we first adopt a definition of cold dark matter, next we discuss under what conditions WIMPs behave as CDM, and then discuss under what conditions axions behave as CDM.

A. Cold dark matter

Astronomical data, in particular data on the cosmic microwave background anisotropies and on the large scale structure of the universe in the linear regime, imply the existence of a new kind of stuff called 'cold dark matter' [1]. What explains the data may technically be called a *perfect fluid with zero pressure* [13]. The state of such a fluid is characterized by a density $\rho(\vec{r}, t)$ and a velocity field $\vec{v}(\vec{r}, t)$. These four degrees of freedom satisfy the continuity equation

$$\partial_t \rho + \vec{\nabla} \cdot (\rho\ \vec{v}) = 0 \tag{2.1}$$

and, in the Newtonian limit of gravity, the equation of motion

$$\partial_t \vec{v} + (\vec{v} \cdot \vec{\nabla})\vec{v} = -\vec{\nabla}\Phi \quad . \tag{2.2}$$

Φ is the gravitational potential. All forces on the CDM fluid other than gravity are assumed to be negligible. The CDM fluid is a source for the gravitational potential:

$$\nabla^2\ \Phi(\vec{r}, t) = 4\pi G(\rho(\vec{r}, t) + ...) \tag{2.3}$$

where the dots represent other sources. The stress-energy-momentum is given by

$$\mathcal{T}^{00} = \rho \quad , \quad \mathcal{T}^{0k} = \rho v^k \quad , \quad \mathcal{T}^{kl} = \rho v^k v^l \quad . \tag{2.4}$$

We will take the above to be the defining properties of CDM because stuff with those properties explains the data mentioned [13]. We will not concern ourselves with the very interesting question to what extent the data demand CDM to be pressureless and collisionless. Instead we want to ask in what limit WIMPs and axions have the properties stated above.

To show that WIMPs or axions behave as CDM it is sufficient to show that, in some average sense, they have the same stress-energy-momentum tensor, Eq. (2.4). Indeed the conservation law $D_\mu \mathcal{T}^{\mu\nu} = 0$ is equivalent in the Newtonian limit to Eqs. (2.1) and (2.2) whereas Einstein's equations imply Eq. (2.3).

For the sake of clarity, let us emphasize that the above is only a good definition of CDM in the linear regime of structure formation. In the non-linear regime CDM produces discrete flows [11, 14] and caustics [3, 4] and these cannot be described by Eqs. (2.1 - 2.3). Instead the state of CDM in the non-linear regime is described by the embedding of a 3-dim. hypersurface in 6-dim. phase space plus the density of particles on this 3-dim. hypersurface. This more general (and hence better) description of CDM defines it as a *cold collisionless fluid*. In the linear regime, the two descriptions are equivalent because the 3-dim. hypersurface covers physical space only once.

B. WIMPs

WIMP dark matter is a (huge) collection of classical point particles. Let their number be N. Their state is given at time t by giving all the particle positions $\vec{r}_i(t)$ and velocities $\vec{v}_i(t)$, $i = 1, 2, ... N$. Their time evolution from appropriate initial conditions is determined by the equations of motion:

$$\frac{d^2\vec{r}_i}{dt^2} = \frac{d\vec{v}_i}{dt} = -\vec{\nabla}\Phi(\vec{r}_i, t) \quad . \tag{2.5}$$

The stress-energy-momentum tensor is

$$(T^{00}\ ,\ T^{0k}\ ,\ T^{kl})(\vec{r}, t) = m_W \sum_{j=1}^{N} (1\ ,\ v_j^k(t)\ ,\ v_j^k(t)v_j^l(t))\delta(\vec{r} - \vec{r}_j(t)) \quad , \tag{2.6}$$

where m_W is the WIMP mass. The indices i and j label the particles whereas $k, l = 1, 2, 3$ label the spatial directions. We want to derive the conditions under which the WIMP particles behave as CDM, defined in the previous subsection. One goes from the one description to the other by averaging over a volume V centered at $\vec{r}$:

$$\begin{aligned}
\rho(\vec{r}, t) &\equiv \mathcal{T}^{00} \equiv \frac{1}{V}\int_V d^3s\ T^{00}(\vec{r} + \vec{s}, t) = \frac{m_W}{V}\int_V d^3s \sum_{j=1}^{N} \delta(\vec{r} + \vec{s} - \vec{r}_j(t)) \\
\vec{\mathcal{P}}(\vec{r}, t) &\equiv \hat{k}\mathcal{T}^{0k} \equiv \frac{1}{V}\int_V d^3s\ \hat{k}\ T^{0k}(\vec{r} + \vec{s}, t) = \frac{m_W}{V}\int_V d^3s \sum_{j=1}^{N} \vec{v}_j(t)\ \delta(\vec{r} + \vec{s} - \vec{r}_j(t)) \\
\mathcal{T}^{kl}(\vec{r}, t) &\equiv \frac{1}{V}\int_V d^3s\ T^{kl}(\vec{r} + \vec{s}, t) = \frac{m_W}{V}\int_V d^3s \sum_{j=1}^{N} v_j^k(t)\ v_j^l(t)\ \delta(\vec{r} + \vec{s} - \vec{r}_j(t)) \quad .
\end{aligned} \tag{2.7}$$

We take V to be time independent. V must be large enough that the fluctuations in particle number inside V are negligible. Conservation of the averaged stress-energy-momentum $\mathcal{T}^{\mu\nu}$ follows merely from the conservation of the original stress-energy-momentum tensor $T^{\mu\nu}$. But $\mathcal{T}^{\mu\nu}$ does not generally have the perfect fluid form. The velocity of the WIMP fluid is

$$\vec{v}(\vec{r}, t) = \frac{1}{\rho(\vec{r}, t)}\vec{\mathcal{P}}(\vec{r}, t) \quad . \tag{2.8}$$

For each particle inside volume V, let us define

$$\Delta\vec{v}_i(\vec{r}, t) \equiv \vec{v}_i(t) - \vec{v}(\vec{r}, t) \quad . \tag{2.9}$$

We have then

$$\mathcal{T}^{kl}(\vec{r}, t) = \rho(\vec{r}, t)\ v^k(\vec{r}, t)\ v^l(\vec{r}, t) + \frac{m_W}{V}\int_V d^3s \sum_{j=1}^{N} \Delta v_j^k\ \Delta v_j^l \delta(\vec{r} + \vec{s} - \vec{r}_j(t)) \quad . \tag{2.10}$$

If the velocity distribution inside V is isotropic, we may define the pressure $p(\vec{r}, t)$ by

$$\frac{m_W}{V}\int_V d^3s \sum_{j=1}^{N} \Delta v_j^k\ \Delta v_j^l \delta(\vec{r} + \vec{s} - \vec{r}_j(t)) \equiv p(\vec{r}, t)\delta^{kl} \tag{2.11}$$

so that

$$\mathcal{T}^{kl} = \rho(\vec{r}, t)\ v^k(\vec{r}, t)\ v^l(\vec{r}, t) + p(\vec{r}, t)\delta^{kl} \quad . \tag{2.12}$$

The stress-energy-momentum tensor is then said to have the perfect fluid form. If, in addition, there is a relation $p(\rho)$ that determines pressure in terms of density (e.g. the relation $p(\rho)$ for atomic gases implied by adiabatic expansion/compression), the conservation laws $D_\mu T^{\mu\nu} = 0$, being four equations for the four unknowns $\rho(\vec{r}, t)$ and $\vec{v}(\vec{r}, t)$, allow us to determine the evolution from arbitrary initial conditions.

As mentioned, CDM is defined to be a *pressureless* perfect fluid. The pressure is a measure of the velocity dispersion of the particles: $p = \frac{\rho}{3} < (\Delta\vec{v})^2 >$. For WIMPs to be CDM, their velocity dispersion must be sufficiently small. The best limit comes from the fact that WIMP density perturbations on scales less than their free streaming distance are erased. Too large a velocity dispersion is inconsistent with the existence of the smallest observed large scale structure, that which gives rise to the 'Lyman-alpha forest' [15]. This constrains the primordial WIMP velocity dispersion to be less than of order $10^{-8}c$ today. If the WIMP particles have ordinary weak interactions, their kinetic energy decouples in the early universe (*i.e.* they stop colliding with other particles in the primordial soup) when the photon temperature is a few MeV [16]. Their velocity dispersion today is then

$$\sqrt{< (\Delta\vec{v})^2 >} \sim 10^{-12}\, c \left(\frac{100 \text{ GeV}}{m_W}\right)^{\frac{1}{2}} \quad . \tag{2.13}$$

The lightest allowed mass is therefore of order keV, which is that of sterile neutrinos [17].

In summary, WIMPs behave as CDM if there exists a volume V large enough so that the fluctuations in particle number inside the volume are negligible, and small enough that the velocity dispersion of the particles inside the volume is negligible. Under these conditions, the WIMPs behave as CDM for any observer who does not resolve length scales smaller than $V^{\frac{1}{3}}$.

Finally, let us remark that gravitational interactions among point particles is a source of velocity dispersion:

$$\Delta v|_g \sim \sqrt{\frac{G m_W}{d_W}} = \sqrt{G\rho}\, d_W \sim 10^{-26} c \left(\frac{m_W}{100 \text{ GeV}}\right)^{\frac{1}{3}} \quad , \tag{2.14}$$

where d_W is the average interparticle distance. It is not possible for the velocity dispersion to be less than $\Delta v|_g$. Furthermore $\Delta v|_g$ grows by gravitational instability as the particles aggregate into clumps of ever increasing size. $\Delta v|_g$ is completely negligible for all proposed WIMP candidates, such as neutralinos and sterile neutrinos. However in present numerical simulations of structure formation the particle mass is 10^4 solar masses or more and hence $\Delta v|_g$ is larger than $4 \cdot 10^{-7}$, which is more than the allowed velocity dispersion of CDM. By this criterion and others [11], present simulations do not have sufficient resolution to describe CDM. For the particles in the simulations to have velocity dispersion as low as that required of CDM, the particle mass should be no more than approximately one solar mass.

C. Axions

In the first part of this subsection, we give the argument why *decoupled* cold axions behave as CDM. Cold axions remain decoupled in the early universe from shortly after their first appearance during the QCD phase transition till the time when gravitational self-interactions cause them to form a BEC. The Bose-Einstein condensation of axions occurs when the photon temperature is approximately 500 eV $\left(\frac{f_a}{10^{12} \text{ GeV}}\right)^{\frac{1}{2}}$ where f_a is the axion decay constant (see Section V). After the condensation is complete, almost all axions are in the same state. In the second part of this subsection, we give the argument why axions behave as CDM when they are all in the same state and that state does not change by rethermalization.

The results obtained in this subsection are not new, although some of the derivations may be. Descriptions of CDM in terms of a classical field are given in Refs. [19–22]. Descriptions of CDM in terms of the Schrödinger equation are given in Refs. [23], [2].

1. Decoupled axions

As mentioned earlier, decoupled axions behave as classical fields because the quantum state occupation numbers of those states that are occupied are huge, of order 10^{61} [2]. In flat space-time, the classical axion field $\phi(\vec{r}, t)$ satisfies the equation of motion

$$(\partial_t^2 - \vec{\nabla}^2 + m^2)\phi = 0 \tag{2.15}$$

where m is the axion mass. Space-time curvature does not play a role in this discusssion, so we ignore it. The stress-energy-momentum tensor is

$$\begin{aligned} T^{00} &= \frac{1}{2}\left(\dot{\phi}^2 + (\vec{\nabla}\phi)^2 + m^2\phi^2\right) \\ \hat{k}T^{0k} &= -\dot{\phi}\vec{\nabla}\phi \\ T^{kl} &= \partial_k\phi\ \partial_l\phi + \frac{1}{2}\left(\dot{\phi}^2 - (\vec{\nabla}\phi)^2 - m^2\phi^2\right)\delta_{kl} \quad . \end{aligned} \tag{2.16}$$

To find out under what conditions decoupled axions behave as CDM, we average again over a spatial volume V located at $\vec{r}$:

$$\mathcal{T}^{\mu\nu}(\vec{r},t) \equiv \frac{1}{V}\int_V d^3s\ T^{\mu\nu}(\vec{r}+\vec{s},t) \quad , \tag{2.17}$$

where $\mu,\nu = 0,1,2,3$. To perform the average, we Fourier transfom ϕ within the volume V:

$$\phi(\vec{x},t) = \sum_{\vec{p}}\ \left(\phi(\vec{p},\vec{r},t)e^{ip\cdot x} + \phi^*(\vec{p},\vec{r},t)e^{-ip\cdot x}\right) \quad , \tag{2.18}$$

where $p\cdot x = -p^0t + \vec{p}\cdot\vec{x}$ and $p^0 = +\sqrt{(\vec{p})^2+m^2}$. The Fourier components depend on the position $\vec{r}$ of the volume. One finds:

$$\begin{aligned} \rho(\vec{r},t) &\equiv \mathcal{T}^{00} = \sum_{\vec{p}}\ N(\vec{p},\vec{r},t)p^0 \\ \vec{\mathcal{P}}(\vec{r},t) &\equiv \hat{k}\mathcal{T}^{0k} = \sum_{\vec{p}}\ N(\vec{p},\vec{r},t)\vec{p} \\ \mathcal{T}^{kl} &= \sum_{\vec{p}}\ N(\vec{p},\vec{r},t)p^kp^l\frac{1}{p^0} \quad , \end{aligned} \tag{2.19}$$

where

$$N(\vec{r},\vec{p},t) = 2p^0|\phi(\vec{p},\vec{r},t)|^2 \quad . \tag{2.20}$$

To obain the expression for $\mathcal{T}^{kl}$ it is necessary to average not only over the volume V, but also over time. The time interval to be averaged over should be much longer than m^{-1}. Eqs. (2.19) show that

$$\mathcal{N}(\vec{r},\vec{p},t) = \frac{V}{(2\pi)^3}N(\vec{r},\vec{p},t) \tag{2.21}$$

may be thought of as the phase space density of the coarse grained axion field.

We assume the axions to be non-relativistic. The average momentum at $\vec{r}$ is $\langle\vec{p}\rangle(\vec{r},t) = \frac{m}{\rho}\vec{\mathcal{P}}$. The classical axion field behaves like CDM provided the momentum distribution $N(\vec{r},\vec{p},t)$ is narrowly peaked around $\langle\vec{p}\rangle(\vec{r},t)$ for all $\vec{r}$. The velocity field is then $\vec{v}(\vec{r},t) = \frac{1}{m}\langle\vec{p}\rangle(\vec{r},t) = \frac{1}{\rho}\vec{\mathcal{P}}$ and

$$\mathcal{T}^{kl}(\vec{r},t) = \rho(\vec{r},t)v^k(\vec{r},t)v^l(\vec{r},t) + \sum_{\vec{p}}N(\vec{r},\vec{p},t)\frac{1}{m}\delta p_k(\vec{r},\vec{p},t)\delta p_l(\vec{r},\vec{p},t) \tag{2.22}$$

where

$$\delta\vec{p}(\vec{r},\vec{p},t) = \vec{p} - \langle\vec{p}\rangle(\vec{r},t) \quad . \tag{2.23}$$

Therefore one condition for decoupled axions to behave as CDM is that they have sufficiently small velocity dispersion. That condition is satisfied for the axions produced during the QCD phase transition. Indeed their velocity dispersion is [see Section V.A]

$$\delta v(t) \sim \frac{1}{mt_1}\frac{a(t_1)}{a(t)} \tag{2.24}$$

where $t_1 \simeq 2 \cdot 10^{-7}\text{sec}\left(\frac{f_a}{10^{12}\ \text{GeV}}\right)^{\frac{1}{3}}$ is the time when the axion mass effectively turns on during the QCD phase transition, and $a(t)$ is the cosmological scale factor. If these axions remained decoupled afterward, their velocity dispersion today would be approximately $5 \cdot 10^{-17}\ c\ \left(\frac{f_a}{10^{12}\ \text{GeV}}\right)^{\frac{5}{6}}$, certainly small enough to be called CDM.

The second condition for decoupled axions to behave as CDM is that they be observed only on length scales larger than their correlation length. The low velocity dispersion of cold decoupled axions implies a correspondingly large correlation length

$$\ell(t) = \frac{1}{m\delta v(t)} \sim t_1 \frac{a(t)}{a(t_1)} \quad . \tag{2.25}$$

On scales less than $\ell(t)$, axions behave differently from CDM. Indeed for CDM, $\rho(\vec{r},t)$ and $\rho(\vec{r}\,',t)$ are independent variables no matter how close $\vec{r}$ and $\vec{r}\,'$, whereas for decoupled axions, $\rho(\vec{r},t)$ and $\rho(\vec{r}\,',t)$ are independent variables only if $|\vec{r}-\vec{r}\,'| > \ell$. However, even today, ℓ is only about $10^{17}\text{cm}\left(\frac{f_a}{10^{12}\ \text{GeV}}\right)^{\frac{1}{6}}$, much smaller than any scale on which we have observational information on the nature of CDM.

2. All axions in the same quantum state

When all the axions are and remain in the same quantum state, the axion fluid also behaves as CDM on all scales of observational interest. The argument for this was given in Ref. [2], but we restate it here for the sake of completeness. Note there is no requirement that the axion state is the lowest energy state. In principle the axion state may be any state. It is important, however, that the axions remain in the same state all the time.

The quantum axion field may be expanded in modes labeled $\vec{\alpha}$:

$$\phi(x) = \sum_{\vec{\alpha}} \left[a_{\vec{\alpha}}\ \Phi_{\vec{\alpha}}(x)\ +\ a^{\dagger}_{\vec{\alpha}}\ \Phi^{*}_{\vec{\alpha}}(x)\right] \tag{2.26}$$

where the $\Phi_{\vec{\alpha}}(x)$ are the positive frequency c-number solutions of the Heisenberg equation of motion for the axion field

$$D^{\mu}D_{\mu}\phi(x) = g^{\mu\nu}[\partial_{\mu}\partial_{\nu} - \Gamma^{\lambda}_{\mu\nu}\partial_{\lambda}]\phi(x) = m^2\phi(x) \quad , \tag{2.27}$$

and the $a_{\vec{\alpha}}$ and $a^{\dagger}_{\vec{\alpha}}$ are annihilation and creation operators satisfying canonical commutation relations. Eqs. (2.27) are written in curved space-time to emphasize that the modes depend on the background. The words 'mode' and 'particle state' are equivalent. Let us assume that, except for a tiny fraction, all axions go to a single particle state with label $\vec{\alpha} = 0$. The corresponding $\Phi_0(x)$ is the axion wavefunction. For the sake of brevity, we call the state of the axion fluid with almost all axions in a single particle state an axion BEC whether or not that particle state is the lowest energy state.

Ignoring the small fraction of axions that are not condensed into mode $\vec{\alpha} = 0$, the state of the axion field is $|N> = (1/\sqrt{N!})\ (a^{\dagger}_0)^N|0>$ where $|0>$ is the empty state, defined by $a_{\vec{\alpha}}\ |0> = 0$ for all $\vec{\alpha}$, and N is the number of axions. The expectation value of the stress-energy-momentum tensor is

$$\mathcal{T}_{\mu\nu}(\vec{r},t) \equiv < N|T_{\mu\nu}|N > = N[\partial_{\mu}\Phi^{*}_0\partial_{\nu}\Phi_0 + \partial_{\nu}\Phi^{*}_0\partial_{\mu}\Phi_0 + g_{\mu\nu}(-\partial_{\lambda}\Phi^{*}_0\partial^{\lambda}\Phi_0 - m^2\Phi^{*}_0\Phi_0)] \quad . \tag{2.28}$$

To see under what conditions the axion BEC behaves as CDM, we may restrict ourselves to Minkowski space-time. Since the axions are non-relativistic, $\Phi_0(x) = e^{-imt}\Psi(x)$ with $\Psi(x)$ slowly varying. Neglecting terms of order $\frac{1}{m}\ \partial_t$ compared to terms of order one, Eq. (2.27) becomes the Schrödinger equation:

$$i\partial_t\Psi = -\frac{\nabla^2}{2m}\Psi \quad . \tag{2.29}$$

The wavefunction may be written as [18]

$$\Psi(\vec{x},t) = \frac{1}{\sqrt{2mN}}B(\vec{x},t)e^{i\beta(\vec{x},t)} \quad . \tag{2.30}$$

In terms of $B(\vec{x},t)$ and $\beta(\vec{x},t)$ the energy and momentum densities are $\mathcal{T}_{00} \equiv \rho = m\left(B(\vec{x},t)\right)^2$ and $\mathcal{T}_{0j} \equiv -\rho v_j = -\left(B(\vec{x},t)\right)^2\partial_j\beta$, in the non-relativistic limit. The velocity field is therefore $\vec{v}(\vec{x},t) = \frac{1}{m}\vec{\nabla}\beta(\vec{x},t)$ [18]. Eq. (2.29) implies the continuity equation, Eq. (2.1), and the equation of motion

$$\partial_t v^k + v^j\partial_j v^k = -\vec{\nabla}q \tag{2.31}$$

where

$$q(\vec{x},t) = -\frac{\nabla^2\sqrt{\rho}}{2m^2\sqrt{\rho}} \quad . \tag{2.32}$$

Following the motion, the stress tensor is

$$T_{jk} = \rho v_j v_k + \frac{1}{4m^2}(\frac{1}{\rho}\partial_j\rho\partial_k\rho - \delta_{jk}\nabla^2\rho) \quad . \tag{2.33}$$

Comparison with Eqs. (2.2) and (2.4) shows that axion BEC differs from CDM: the last terms on the RHS of Eqs. (2.31) and (2.33) are absent in the CDM case.

The extra terms are due to the Heisenberg uncertainty principle. When one attempts to localize the axion BEC within a region of size D, the axions acquire a minimum momentum spread of order $\Delta p \sim \hbar/D$ and hence a velocity dispersion $\Delta v \sim \hbar/mD$. The axion BEC tends therefore to delocalize. The tendency to delocalize is described by the force per unit mass $-\vec{\nabla}q$ appearing in Eq. (2.31), and by the extra stresses in Eq. (2.33). CDM has no such tendency to delocalize. Whether this difference between axion BEC and CDM is of observational relevance depends on the axion mass m. The properties of CDM have been observed only on very large scales, $D \gtrsim 100$ kpc. The associated velocity dispersion is tiny, of order $3 \cdot 10^{-24}\ c\ \left(\frac{10^{-5}\ \mathrm{eV}}{m}\right)$, for the axion masses of interest to us. Hence there is no distinction between axion BEC and CDM, on scales of observational interest, which follows from the extra delocalizing forces on the axion BEC. As an illustration, consider the equation for the evolution of axion BEC density perturbations in the matter dominated phase of the expanding universe [21] [2, 22]:

$$\partial_t^2\delta + 2H\partial_t\delta - \left(4\pi G\rho_0 - \frac{k^4}{4m^2a^4}\right)\delta = 0 \quad . \tag{2.34}$$

Here, $H \equiv \dot{a}/a$ is the Hubble expansion rate, $a(t)$ the scale factor, ρ_0 the average density of the axion BEC (assumed to be the dominant form of matter), $\vec{k}$ the co-moving wavevector, and δ the Fourier component of $(\rho - \rho_0)/\rho_0$ with wavevector $\vec{k}$. The last term in Eq. (2.34) is absent for CDM. As a result of this term, whereas the Jeans length of CDM vanishes, axion BEC has Jeans length [21] [2, 22]:

$$k_{\mathrm{J}}^{-1} = (16\pi G\rho m^2)^{-\frac{1}{4}} = 1.02 \cdot 10^{14}\ \mathrm{cm}\left(\frac{10^{-5}\ \mathrm{eV}}{m}\right)^{\frac{1}{2}}\left(\frac{10^{-29}\ \mathrm{g/cm^3}}{\rho}\right)^{\frac{1}{4}} \quad . \tag{2.35}$$

It is small compared to the smallest scales (~ 100 kpc) for which we have observations on the behavior of CDM.

Several authors have proposed [24] that the dark matter is a Bose-Einstein condensate of particles with mass of order 10^{-22} eV. When the mass is that small, the dark matter BEC behaves differently from CDM on scales of observational interest as a result of the tendency of the BEC to delocalize. We are not considering this interesting possibility here because axion masses are not expected to be so small.

In summary, cold axions with mass in the 10^{-5} range (give or take a few orders of magnitude) behave as CDM on all scales of observational interest in two different cases: 1) when they are decoupled and therefore behave as a classical field, and 2) when they are all in the same particle state. The latter result constrains the conditions under which axion BEC may differ from CDM. For the axion BEC to differ from CDM it must be rethermalizing, i.e. the state that most axions are in must be changing in time, as when it tracks the lowest energy available state.

III. AXION FIELD DYNAMICS

We consider two types of processes through which dark matter axions may thermalize in the early universe: self-interactions of the $\lambda\phi^4$ type and gravitational self-interactions. We will see in Section V, confirming the results of Ref. [2], that the $\lambda\phi^4$ interaction is barely effective in thermalizing axions for a brief period just after they are produced during the QCD phase transition, whereas gravitational self-interactions are clearly effective in thermalizing axions after the photon temperature reaches approximately 500 eV $\left(\frac{f_a}{10^{12}\ \mathrm{GeV}}\right)^{\frac{1}{2}}$. When the axions thermalize, they form a Bose-Einstein condensate.

In this Section, we first express the axion field dynamics in terms of a set of coupled oscillators. Next we obtain the evolution equations for the oscillator occupation numbers up to second order in perturbation theory. We show that the second order terms yield the usual Boltzmann equation for the evolution of the momentum distribution provided

that the transition rate between momentum states is small compared to their spread in energy: $\Gamma << \delta\omega$. This latter condition defines the 'particle kinetic regime'. In the particle kinetic regime, the first order terms in the evolution equations are irrelevant because they average out in time. Dark matter axions are, however, in the opposite regime: $\delta\omega << \Gamma$, which we refer to as the 'condensed regime'. In the condensed regime, the first order terms do not average out in time and dominate over the second order terms. Using the first order equations, we give expressions estimating the relaxation rate of the axion dark matter momentum distribution due to $\lambda\phi^4$ self-interactions and to gravitational self-interactions.

A. Axion interactions

Including lowest order self-interactions but neglecting gravity, the action density of axions is

$$\mathcal{L}_a = -\frac{1}{2}\partial_\mu\phi\partial^\mu\phi - \frac{1}{2}m^2\phi^2 + \frac{\lambda}{4!}\phi^4 + ... \quad . \tag{3.1}$$

The dots represent interactions of the axion with other particles and axion self-interactions which are higher order in an expansion in powers of ϕ. For the axion that solves the strong CP problem [25–27], the mass m and self-coupling λ are given by

$$\begin{aligned} m &= \frac{m_\pi f_\pi}{f_a}\frac{\sqrt{m_u\ m_d}}{m_u+m_d} \simeq 6\cdot 10^{-6}\text{eV}\ \frac{10^{12}\ \text{GeV}}{f_a} \\ \lambda &= \frac{m^2}{f_a^2}\frac{m_u^3+m_d^3}{(m_u+m_d)^3} \simeq 0.35\ \frac{m^2}{f_a^2} \end{aligned} \tag{3.2}$$

where f_a is the axion decay constant, m_π the pion mass, $f_\pi \simeq 93$ MeV the pion decay constant, and m_u and m_d the up and down quark masses. The formula for the axion mass [26] is obtained by expanding the effective potential for pions and axions to second order in the physical axion field. To obtain λ, simply expand to fourth order.

We introduce a cubic box of volume $V = L^3$ with periodic boundary conditions at its surface. Inside the box, the axion field $\phi(\vec{x},t)$ and its canonical conjugate field $\pi(\vec{x},t)$ are expanded into Fourier components

$$\begin{aligned} \phi(\vec{x},t) &= \sum_{\vec{n}}\left(a_{\vec{n}}(t)\ \Phi_{\vec{n}}(\vec{x}) \ + \ a^\dagger_{\vec{n}}(t)\ \Phi^*_{\vec{n}}(\vec{x})\right) \\ \pi(\vec{x},t) &= \sum_{\vec{n}}(-i\omega_{\vec{n}})\left(a_{\vec{n}}(t)\ \Phi_{\vec{n}}(\vec{x}) \ - \ a^\dagger_{\vec{n}}(t)\ \Phi^*_{\vec{n}}(\vec{x})\right) \end{aligned} \tag{3.3}$$

where

$$\Phi_{\vec{n}}(\vec{x}) = \frac{1}{\sqrt{2\omega_{\vec{n}}V}}\ e^{i\vec{p}_{\vec{n}}\cdot\vec{x}} \qquad , \tag{3.4}$$

and $\vec{n} = (n_1, n_2, n_3)$ with n_k $(k = 1, 2, 3)$ integers, $\vec{p}_{\vec{n}} = \frac{2\pi}{L}\vec{n}$, and $\omega = \sqrt{\vec{p}\cdot\vec{p} + m^2}$. The $a_{\vec{n}}$ and $a^\dagger_{\vec{n}}$ satisfy canonical equal-time commutation relations:

$$[a_{\vec{n}}(t), a^\dagger_{\vec{n}'}(t)] = \delta_{\vec{n},\vec{n}'} \quad , \quad [a_{\vec{n}}(t), a_{\vec{n}'}(t)] = 0 \quad . \tag{3.5}$$

Note that we are quantizing in the Heisenberg picture, not the interacting picture.

Provided the axions are non-relativistic, the Hamiltonian is

$$H = \sum_{\vec{n}}\omega_{\vec{n}}\ a^\dagger_{\vec{n}}a_{\vec{n}} \ + \sum_{\vec{n}_1,\vec{n}_2,\vec{n}_3,\vec{n}_4}\frac{1}{4}\ \Lambda_s{}^{\vec{n}_3,\vec{n}_4}_{\vec{n}_1,\vec{n}_2}\ a^\dagger_{\vec{n}_1}a^\dagger_{\vec{n}_2}a_{\vec{n}_3}a_{\vec{n}_4} \tag{3.6}$$

where

$$\Lambda_s{}^{\vec{n}_3,\vec{n}_4}_{\vec{n}_1,\vec{n}_2} = -\frac{\lambda}{4m^2V}\ \delta_{\vec{n}_1+\vec{n}_2,\vec{n}_3+\vec{n}_4} \quad . \tag{3.7}$$

The presence of the Kronecker symbol $\delta_{\vec{n}_1+\vec{n}_2,\vec{n}_3+\vec{n}_4}$ expresses momentum conservation for each individual interaction. In Eq. (3.6) we dropped all terms of the form $a^\dagger a^\dagger a^\dagger a^\dagger$, $a\ a^\dagger\ a^\dagger\ a^\dagger$, $a\ a\ a\ a$, and $a\ a\ a\ a^\dagger$. We are justified in doing so because these operators violate axion number and therefore allow, in lowest order, only processes (such as

$a + a + a \to a$) that are forbidden by energy-momentum conservation. In higher orders, these operators allow axion number violating, energy-momentum conserving processes (such as $a + a + a + a \to a + a$) but at too small a rate to be relevant. In fact, all axion number violating processes, including the axion decay to two photons, occur only on time scales much longer than the age of the universe in the axion mass range (10^{-5} eV) of interest.

In the Newtonian limit, the gravitational self-interactions of the axion fluid are described by

$$H_g = -\frac{G}{2}\int d^3x\ d^3x'\ \frac{\rho(\vec{x},t)\rho(\vec{x}',t)}{|\vec{x}-\vec{x}'|} \tag{3.8}$$

where $\rho = \frac{1}{2}(\pi^2 + m^2\phi^2)$ is the axion energy density. Because we neglect general relativistic corrections, our conclusions are applicable only for processes that take place well within the horizon. Substituting ϕ and π by their expansions in terms of creation and annihilation operators, Eqs. (3.3), and dropping again all axion number violating terms, Eq. (3.8) becomes

$$H_g = \sum_{\vec{n}_1,\vec{n}_2,\vec{n}_3,\vec{n}_4} \frac{1}{4}\ \Lambda_g{}^{\vec{n}_3,\vec{n}_4}_{\vec{n}_1,\vec{n}_2}\ a^\dagger_{\vec{n}_1} a^\dagger_{\vec{n}_2} a_{\vec{n}_3} a_{\vec{n}_4} \tag{3.9}$$

where

$$\Lambda_g{}^{\vec{n}_3,\vec{n}_4}_{\vec{n}_1,\vec{n}_2} = -\frac{4\pi G m^2}{V}\delta_{\vec{n}_1+\vec{n}_2,\vec{n}_3+\vec{n}_4}\ \left(\frac{1}{|\vec{p}_{\vec{n}_1}-\vec{p}_{\vec{n}_3}|^2}+\frac{1}{|\vec{p}_{\vec{n}_1}-\vec{p}_{\vec{n}_4}|^2}\right) \quad . \tag{3.10}$$

Having expressed the dynamics of the axion field in terms of coupled oscillators, we now study the time evolution of such systems.

B. Evolution equations

We just saw that the axion field is equivalent to a large number M of coupled oscillators with Hamiltonian of the form

$$H = \sum_{j=1}^{M}\ \omega_j a_j^\dagger a_j\ +\ \sum_{i,j,k,l}\ \frac{1}{4}\ \Lambda^{ij}_{kl}\ a^\dagger_k a^\dagger_l a_i a_j \quad . \tag{3.11}$$

In particular, the total number of quanta

$$N = \sum_{j=1}^{M} a_j^\dagger a_j \tag{3.12}$$

is conserved. In Eq. (3.11), $\Lambda^{ij}_{kl} = \Lambda^{ij}_{lk} = \Lambda^{ji}_{kl} = \Lambda^{kl}_{ij}$ *. The question of interest now is the following: starting with an arbitrary initial state, how quickly will the averages $\langle\mathcal{N}_k\rangle$ of the oscillator occupation numbers $\mathcal{N}_k = a^\dagger_k a_k$ approach a thermal distribution? The usual approach to this question uses the Boltzmann equation. However, we will see that the assumptions underlying the Boltzmann equation are not valid for the cold axion fluid. So we need a more general approach.

It is instructive to start with a system of just four oscillators ($M = 4$) and one interaction between them:

$$H = \sum_{j=1}^{4}\omega_j a_j^\dagger a_j + \Lambda(a_1^\dagger a_2^\dagger a_3 a_4 + a_3^\dagger a_4^\dagger a_1 a_2) \quad . \tag{3.13}$$

We have in this case

$$\dot{a}_1 = i[H, a_1] = i(-\omega_1 a_1 - \Lambda a_2^\dagger a_3 a_4) \tag{3.14}$$

and therefore

$$\dot{\mathcal{N}}_1 = i\Lambda(a_1 a_2 a_3^\dagger a_4^\dagger - a_1^\dagger a_2^\dagger a_3 a_4) \tag{3.15}$$

and similar equations for the other $\dot{a}_j$ and $\dot{\mathcal{N}}_j$. We solve the equations perturbatively up to $\mathcal{O}(\Lambda^2)$. Let us define

$$a_j(t) = (A_j + B_j(t))e^{-i\omega_j t} + \mathcal{O}(\Lambda^2) \tag{3.16}$$

where $A_j \equiv a_j(0)$ and $B_j(t)$ are respectively zeroth and first order, and $B_j(0) = 0$. Eq. (3.14) implies

$$\dot{B}_1 = -i\Lambda A_2^\dagger A_3 A_4 e^{+i\Omega t} + \mathcal{O}(\Lambda^2) \quad , \tag{3.17}$$

with $\Omega \equiv \omega_1 + \omega_2 - \omega_3 - \omega_4$, and therefore

$$B_1(t) = -i\Lambda A_2^\dagger A_3 A_4 \; e^{+i\Omega t/2} \; \frac{2}{\Omega}\sin(\frac{\Omega t}{2}) + \mathcal{O}(\Lambda^2) \quad . \tag{3.18}$$

Substituting this into Eq. (3.15), we have

$$\begin{aligned}
\dot{\mathcal{N}}_1 &= i\Lambda(A_1 A_2 A_3^\dagger A_4^\dagger e^{-i\Omega t} - h.c.) \\
&+ \Lambda^2[(A_2^\dagger A_2 A_3 A_3^\dagger A_4 A_4^\dagger + A_1 A_1^\dagger A_3 A_3^\dagger A_4 A_4^\dagger \\
&- A_1 A_1^\dagger A_2 A_2^\dagger A_4 A_4^\dagger - A_1 A_1^\dagger A_2 A_2^\dagger A_3^\dagger A_3) e^{-i\Omega t/2} \; \frac{2}{\Omega}\sin(\frac{\Omega t}{2}) + h.c.] \; + \; \mathcal{O}(\Lambda^3) \; .
\end{aligned} \tag{3.19}$$

Eq. (3.19) may be recast in the form

$$\begin{aligned}
\dot{\mathcal{N}}_1 &= i\Lambda(A_1 A_2 A_3^\dagger A_4^\dagger e^{-i\Omega t} - h.c.) \\
&+ \Lambda^2 \left[\mathcal{N}_3\mathcal{N}_4(\mathcal{N}_1+1)(\mathcal{N}_2+1) - \mathcal{N}_1\mathcal{N}_2(\mathcal{N}_3+1)(\mathcal{N}_4+1)\right] \frac{2}{\Omega}\sin(\Omega t) \; + \; \mathcal{O}(\Lambda^3)
\end{aligned} \tag{3.20}$$

by rewriting the second order terms.

We now generalize to a system with an arbitrarily large number M of coupled oscillators, Eqs. (3.11). The calculation is essentially the same as for the $M = 4$ toy model, except that there is a multiplicity of interaction terms to keep track of. One finds ($l = 1...M$)

$$\begin{aligned}
\dot{\mathcal{N}}_l &= i \sum_{i,j,k=1}^{M} \frac{1}{2}(\Lambda_{ij}^{kl} A_i^\dagger A_j^\dagger A_k A_l e^{-i\Omega_{ij}^{kl} t} - h.c.) \\
&+ \sum_{k,i,j=1}^{M} \frac{1}{2}|\Lambda_{ij}^{kl}|^2 \left[\mathcal{N}_i\mathcal{N}_j(\mathcal{N}_l+1)(\mathcal{N}_k+1) - \mathcal{N}_l\mathcal{N}_k(\mathcal{N}_i+1)(\mathcal{N}_j+1)\right] \frac{2}{\Omega_{ij}^{kl}}\sin(\Omega_{ij}^{kl} t) \\
&+ \sum_{k,i,j=1}^{M} \sum_{\substack{p,m,n=1 \\ (p;m,n)\neq(k;i,j)}}^{M} [\frac{1}{2}\Lambda_{kl}^{ij}\Lambda_{mn}^{lp} A_m^\dagger A_n^\dagger A_k^\dagger A_p A_i A_j e^{i(\Omega_{ij}^{kl}+\Omega_{lp}^{mn}/2)t} \; \frac{1}{\Omega_{lp}^{mn}}\sin(\frac{\Omega_{lp}^{mn}}{2}t) + h.c.] \\
&+ \sum_{k,i,j=1}^{M} \sum_{\substack{p,m,n=1 \\ (p;m,n)\neq(l;i,j)}}^{M} [\frac{1}{2}\Lambda_{kl}^{ij}\Lambda_{mn}^{kp} A_l^\dagger A_m^\dagger A_n^\dagger A_p A_i A_j e^{i(\Omega_{ij}^{kl}+\Omega_{kp}^{mn}/2)t} \; \frac{1}{\Omega_{kp}^{mn}}\sin(\frac{\Omega_{kp}^{mn}}{2}t) + h.c.] \\
&- \sum_{k,i,j=1}^{M} \sum_{\substack{p,m,n=1 \\ (p;m,n)\neq(j;l,k)}}^{M} [\frac{1}{2}\Lambda_{lk}^{ij}\Lambda_{ip}^{mn} A_l^\dagger A_k^\dagger A_p^\dagger A_m A_n A_j e^{i(\Omega_{ij}^{kl}+\Omega_{mn}^{ip}/2)t} \; \frac{1}{\Omega_{mn}^{ip}}\sin(\frac{\Omega_{mn}^{ip}}{2}t) + h.c.] \\
&- \sum_{k,i,j=1}^{M} \sum_{\substack{p,m,n=1 \\ (p;m,n)\neq(i;l,k)}}^{M} [\frac{1}{2}\Lambda_{lk}^{ij}\Lambda_{jp}^{mn} A_l^\dagger A_k^\dagger A_p^\dagger A_i A_m A_n e^{i(\Omega_{ij}^{kl}+\Omega_{mn}^{jp}/2)t} \; \frac{1}{\Omega_{mn}^{jp}}\sin(\frac{\Omega_{mn}^{jp}}{2}t) + h.c.] \\
&+ \mathcal{O}(\Lambda^3) \quad ,
\end{aligned} \tag{3.21}$$

where $\Omega_{ij}^{kl} \equiv \omega_k + \omega_l - \omega_i - \omega_j$. The double sums are absent in the toy model because there is only one interaction in that case. At any rate, the double sums will not play an important role in the discussion that follows.

C. The particle kinetic regime

The interaction terms cause transitions in which a quantum is moved from oscillator j to oscillator k and at the same time a quantum is moved from oscillator i to oscillator l. As a general rule, energy is not conserved in any one transition. Only the total energy of the fluid is conserved. However, for the oscillator couplings of the axion field case, Eqs. (3.7) and (3.10), three-momentum is conserved in each transition.

In almost all systems of physical interest, the rate at which the occupation number of a typical system oscillator changes is small compared to the energy exchanged in the transitions it makes, i.e. $\Omega_{ij}^{kl} t >> 1$. This condition defines the 'particle kinetic regime'. In the particle kinetic regime, the first order terms in Eq. (3.21), as well as the second order terms in the double sums, average to zero in time. In addition, energy is conserved in each transition because

$$\frac{2}{\Omega_{ij}^{kl}} \sin(\Omega_{ij}^{kl}\ t) \to 2\pi\delta(\Omega_{ij}^{kl}) \tag{3.22}$$

for $\Omega_{ij}^{kl}\ t \to \infty$. We have then

$$< \dot{\mathcal{N}}_l >= + \sum_{i,j,k=1}^{M} \frac{1}{2}|\Lambda_{ij}^{kl}|^2 \left[\mathcal{N}_i\mathcal{N}_j(\mathcal{N}_l+1)(\mathcal{N}_k+1) - \mathcal{N}_l\mathcal{N}_k(\mathcal{N}_i+1)(\mathcal{N}_j+1)\right] 2\pi\delta(\Omega_{ij}^{kl}) \quad . \tag{3.23}$$

Note that the average on the LHS of this equation is a time average, not a quantum-mechanical average. Eq. (3.23) is valid as an operator statement.

If we substitute for the oscillator couplings those, Eq. (3.7), implied by $\lambda\phi^4$ self-interactions and take the infinite volume limit, we recover the Boltzmann equation [28] as an operator statement:

$$\begin{aligned} < \dot{\mathcal{N}}_1 > \ &= \ \frac{1}{2\omega_1}\int \frac{d^3p_2}{(2\pi)^3 2\omega_2}\int \frac{d^3p_3}{(2\pi)^3 2\omega_3}\int \frac{d^3p_4}{(2\pi)^3 2\omega_4} \\ &\lambda^2 \ \ (2\pi)^4\delta^4(p_1+p_2-p_3-p_4)\ \frac{1}{2} \\ &\quad [(\mathcal{N}_1+1)(\mathcal{N}_2+1)\mathcal{N}_3\mathcal{N}_4 - \mathcal{N}_1\mathcal{N}_2(\mathcal{N}_3+1)(\mathcal{N}_4+1)] \end{aligned} \tag{3.24}$$

including the factor (explicitly shown) of 1/2 for identical particles in the final state. In Eq. (3.24), $\mathcal{N}_k$ is short for $\mathcal{N}_{\vec{p}_k}$. The $a + a \to a + a$ scattering cross-section due to the $\lambda\phi^4$ self-interaction is

$$\begin{aligned} \sigma_\lambda \ &= \ \frac{1}{|\vec{v}_1 - \vec{v}_2|}\frac{1}{2\omega_1}\frac{1}{2\omega_2}\int \frac{d^3p_3}{(2\pi)^3 2\omega_3}\int \frac{d^3p_4}{(2\pi)^3 2\omega_4}\lambda^2\frac{1}{2}(2\pi)^4\delta^4(p_1+p_2-p_3-p_4) \\ &= \ \frac{\lambda^2}{64\pi}\frac{1}{m^2} \end{aligned} \tag{3.25}$$

where the last equality holds in the non-relativistic limit. The particle density in physical space is

$$n = \int \frac{d^3p}{(2\pi)^3}\mathcal{N}_{\vec{p}} \quad . \tag{3.26}$$

If most states are not occupied, Eqs. (3.24),(3.25) and (3.26) imply the usual expression for the relaxation rate

$$\Gamma \sim \frac{\dot{\mathcal{N}}}{\mathcal{N}} \sim n\ \sigma\ \delta v \tag{3.27}$$

where δv is a measure of the velocity dispersion in the fluid.

However, in the case of cold dark matter axions, the momentum states that are occupied are enormously occupied [2]: $\mathcal{N}_{\vec{p}} \sim 10^{61}\ \left(\frac{f}{10^{12}\ \mathrm{GeV}}\right)^{\frac{8}{3}}$ for $p \lesssim p_{\max}(t) \sim \frac{1}{t_1}\frac{a(t_1)}{a(t)}$; see Section V. For such a situation, consider the factor

$$F(\mathcal{N}) \equiv (\mathcal{N}_1+1)(\mathcal{N}_2+1)\mathcal{N}_3\mathcal{N}_4 - \mathcal{N}_1\mathcal{N}_2(\mathcal{N}_3+1)(\mathcal{N}_4+1) \tag{3.28}$$

that appears in Eq. (3.24). The first term in $F(\mathcal{N})$ multiplies the contribution to $< \dot{\mathcal{N}}_1 >$ from $a(p_1) + a(p_2) \leftarrow a(p_3) + a(p_4)$ transitions whereas the second terms multiplies the contribution from $a(p_1) + a(p_2) \to a(p_3) + a(p_4)$. By energy conservation, if the initial particle states (e.g. $\vec{p}_1$ and $\vec{p}_2$) are both highly occupied, the final particle states ($\vec{p}_3$ and $\vec{p}_4$) are almost always highly occupied as well. The RHS of Eq. (3.24) is dominated by regions of momentum space where all four $\mathcal{N}_k$ are of order $\mathcal{N} \sim 10^{61}$. The rate for $a(p_1) + a(p_2) \to a(p_3) + a(p_4)$ transitions, per pair of initial state particles, is multiplied by $(\mathcal{N}_3+1)(\mathcal{N}_4+1) \sim \mathcal{N}^2$ compared to the case where most states are empty. However, the rate for $a(p_1) + a(p_2) \leftarrow a(p_3) + a(p_4)$ is similarly multiplied by order $\mathcal{N}^2$. The two cancel each other since the terms of order $\mathcal{N}^4$ cancel out in $F(\mathcal{N})$. However, the order $\mathcal{N}^3$ terms do not cancel out. The upshot is that,

although the rates at which quanta enter and leave any one state $\vec{p}_1$ are both enhanced factors of $\mathcal{N}^2$, the difference between those two rates, i.e. the relaxation rate, is multiplied by one factor of $\mathcal{N}$:

$$\Gamma \sim \frac{\dot{\mathcal{N}}}{\mathcal{N}} \sim n\ \sigma\ \delta v\ \mathcal{N} \quad . \tag{3.29}$$

Using this equation, we show in Section V that cold axions barely thermalize near time t_1, just after they are produced during the QCD phase transition. However the condition $\Gamma << \delta\omega$ that defines the particle kinetic regime is only borderline satisfied at time t_1 and is violated afterward. Shortly after t_1 the axion fluid enters the condensed regime. Relaxation in the condensed regime is discussed in the next subsection.

We would like to conclude this subsection with remarks about gravitational interactions. It has long been recognized that gravitational interactions do not fit into the usual discussion of thermalization [29]. Indeed the total cross section for gravitational scattering is formally infinite, and Eqs. (3.27) and (3.29) are clearly invalid. Let's use our derivation of the Boltzmann equation to shed some light on this matter. Eq. (3.21) is valid for all interactions since it only assumes the ordinary rules of quantum mechanics. However, Eq. (3.23) is valid only in the particle kinetic regime. It does not apply to transitions with very small momentum, and hence very small energy, transfer since the particle kinetic condition $\Omega_{ij}^{kl}\ t >> 1$ is violated then. The divergence in the cross-section for gravitational scattering is at small momentum transfers (forward scattering), where the assumptions underlying the calculation of the cross-section are invalid. Even the notion of scattering is dubious there. We should restrict the sum in Eq. (3.23) to transitions that are in the particle kinetic regime. This will cut off the divergence in the total cross section for gravitational scattering but the differential cross section will still be peaked in the forward direction. Forward scattering has only limited effectiveness in relaxing a momentum distribution since the particle momenta change only a little bit at the time. The cross section appearing in Eqs. (3.27) and (3.29) is the cross-section for large angle scattering since only large angle scattering has an immediate effect on the momentum distribution. The issue does not arise for $\lambda\phi^4$ interactions because the differential cross-section is not sharply peaked in the forward direction in that case. We conclude that one may use Eq. (3.27) or (3.29) with

$$\sigma_g \sim \frac{4G^2m^2}{(\delta v)^4} \tag{3.30}$$

to estimate the relaxation rate by gravitational scattering in the particle kinetic regime.

D. The condensed regime

Consider a huge number N of particles occupying a small number K of states. The average occupation number of those states that are highly occupied is $\mathcal{N} = \frac{N}{K} >> 1$. Assume that the energy spread of the highly occupied states is small compared to the evolution rate (to be determined) of the system: $\delta\omega << \Gamma$. For transitions between such closely spaced states,

$$e^{-i\Omega_{ij}^{kl}t} = 1 \tag{3.31}$$

in Eq. (3.21). The first order terms in that equation no longer average to zero. We want to estimate the relaxation rate under these conditions.

It may appear at first that we are embarking on a meaningless quest because the condition $\Omega_{ij}^{kl}t << 1$ implies that the energy difference between highly occupied states is too small for anyone to tell whether a particle has made a transition from one highly occupied state to another in time t. That is indeed so. However, for the case of interest to us, $(\Omega_{ij}^{kl}t)\mathcal{N} >> 1$ and it is therefore meaningful to ask whether of order $\mathcal{N}$ particles have made a transition between highly occupied states. The latter is the question which is relevant to estimating the relaxation rate.

Let us define $c_l(t) \equiv a_l(t)e^{i\omega_l t}$. The Hamiltonian (3.11) implies

$$\dot{c}_l(t) = -i \sum_{k,i,j=1}^{M} \frac{1}{2}\ \Lambda_{kl}^{ij}\ c_k^\dagger c_i c_j e^{i\Omega_{ij}^{kl}t} \quad . \tag{3.32}$$

Let us define further

$$c_l(t) \equiv C_l(t) + d_l(t) \tag{3.33}$$

where the $d_l(t)$, like the $c_l(t)$, are annihilation operators satisfying canonical equal time commutation relations and the $C_l(t)$ are complex c-number functions which satisfy the classical equations of motion

$$\dot{C}_l(t) = -i \sum_{k,i,j=1}^{M} \frac{1}{2}\Lambda_{kl}^{ij}\ C_k^* C_i C_j e^{i\Omega_{ij}^{kl}t} \quad . \tag{3.34}$$

For the highly occupied cold axion states, the C_l have magnitude of order $\sqrt{\mathcal{N}}$. The relaxation rate of the highly condensed cold axions is the inverse of the time scale over which those $C_l(t)$ change by order $\sqrt{\mathcal{N}}$.

Since the sum in Eq. (3.34) is dominated by terms for which k, i and j label highly occupied axion states,

$$\dot{C}_l(t) \sim -i \sum_{k,i,j=1}^{K} \frac{1}{2}\Lambda_{kl}^{ij}\ C_k^* C_i C_j \quad . \tag{3.35}$$

For $\lambda\phi^4$ self-interactions, we substitute Eq. (3.7). This yields

$$\dot{C}_{\vec{p}_1}(t) \sim +i\frac{\lambda}{4m^2V} \sum_{\vec{p}_2,\vec{p}_3} \frac{1}{2} C^*_{\vec{p}_2} C_{\vec{p}_3} C_{\vec{p}_4} \tag{3.36}$$

where $\vec{p}_4 = \vec{p}_1 + \vec{p}_2 - \vec{p}_3$, and the sum is restricted to the K highly occupied states for which $p \lesssim p_{\rm max}$. We may think of the terms on the RHS of Eq. (3.36) as steps in a random walk in complex space. The magnitude of each step is of order $\mathcal{N}^{\frac{3}{2}}$ and the number of steps is of order K^2. Hence

$$\dot{C}_{\vec{p}} \sim \frac{\lambda}{4m^2V} K\mathcal{N}^{\frac{3}{2}} \sim \frac{\lambda}{4m^2V} N\mathcal{N}^{\frac{1}{2}} \quad . \tag{3.37}$$

Hence our estimate for the relaxation rate due to $\lambda\phi^4$ self-interactions in the condensed regime [2]:

$$\Gamma_\lambda \sim \frac{1}{4} n\lambda m^{-2} \tag{3.38}$$

where $n = N/V$ is the density of particles in the highly occupied closely spaced states. Likewise, using Eq. (3.10), we find that through gravitational self-interactions

$$\dot{C}_{\vec{p}_1}(t) \sim +i\frac{4\pi G m^2}{V} \sum_{\vec{p}_2,\vec{p}_3} \frac{1}{2} C^*_{\vec{p}_2} C_{\vec{p}_3} C_{\vec{p}_4} \left(\frac{1}{|\vec{p}_1 - \vec{p}_3|^2} + \frac{1}{|\vec{p}_1 - \vec{p}_4|^2} \right) \quad . \tag{3.39}$$

The corresponding relaxation rate is

$$\Gamma_g \sim 4\pi G n m^2 \ell^2 \tag{3.40}$$

where $\ell \sim \frac{1}{p_{\rm max}}$ is the correlation length of the particles.

We note that at the boundary between the particle kinetic and condensed regimes, where $\delta\omega \sim \Gamma$, the two estimates of the relaxation rate agree with one another. Indeed at that boundary, up to factors of order two or so,

$$\delta v\ \mathcal{N} \sim \delta v \frac{n}{(\delta p)^3} \sim \frac{n}{m^2\delta\omega} \sim \frac{n}{m^2\Gamma} \quad . \tag{3.41}$$

Substituting this into Eq. (3.29) for the relaxation rate due to $\lambda\phi^4$ self-interactions in the particle kinetic regime yields Eq. (3.38) which is the corresponding estimate in the condensed regime. The same holds true for the gravitational self-interactions.

Let us also note that Eqs. (3.38) and (3.40) are not valid when almost all axions are in a single state ($K = 1$), as when the Bose-Einstein condensation has been completed. Indeed, if $K = 1$, there is only one term in the sum on the RHS of Eqs. (3.36) and (3.39) that is enhanced by large occupation numbers, i.e. the term for which both $\vec{p}_2$ and $\vec{p}_3$ equal the momentum of the single highly occupied state, and it describes an interaction with zero momentum transfer. Thus, once the Bose-Einstein condensation is complete and all axions are in the lowest energy state, any further thermalization is suppressed.

Finally consider transitions $a(\vec{p}_1) + a(\vec{p}_2) \leftrightarrow a(\vec{p}_3) + a(\vec{p}_4)$ where $\vec{p}_2$ and $\vec{p}_4$ are momenta of highly occupied states but $\vec{p}_1$ and $\vec{p}_3$ are not. Such transitions are in the condensed regime because the momentum transfer, and hence the energy transfer, is small. Eqs. (3.36) and (3.39) apply to such transitions and imply that the rate at which states with

$p > p_{\max}$ modify their occupation numbers is also given by Eqs. (3.38) and (3.40) with the proviso that the quanta can only move between states differing in momentum by less than $p_{\max}$.

Eq. (3.40) has a simple interpretation. The axions, having energy density $\rho = mn$ and correlation length ℓ, produce gravitational fields $g \sim 4\pi G\rho\ell$. The gravitational force on a particle is of order $g\omega$, where ω is the energy of the particle. Since the force is the rate of change of the particle's momentum, the relaxation rate is of order

$$\Gamma_g \sim \frac{g\omega}{\Delta p} \sim 4\pi G n m \ell \frac{\omega}{\Delta p} \tag{3.42}$$

where Δp is the momentum dispersion of the particles. For the axions themselves, we obtain the relaxation rate Eq. (3.40) by substituting $\omega = m$ and $\Delta p \sim \ell^{-1}$. Eq. (3.42) shows that the momentum distribution of any particle species is modified by the gravitational fields of the cold axion fluid and therefore that gravitational interactions may produce thermal contact between the cold axions and other particle species. This is discussed in the next subsection.

E. Other species

Our purpose in this subsection is to estimate the gravitational interaction rates of other species - baryons, relativistic axions and photons - with the cold axion fluid. We are motivated by the question, discussed in Section V, whether these other species come into thermal contact with the cold axion fluid.

The Hamiltonian describing gravitational interactions between the cold axions and any other species has the general form:

$$H = \sum_{j=1}^{M} \omega_j a_j^\dagger a_j \;+\; \sum_{r=1}^{S} \omega_r b_r^\dagger b_r \;+\; \sum_{i,j,k,l} \frac{1}{4}\, \Lambda_{kl}^{ij}\; a_k^\dagger a_l^\dagger a_i a_j \;+\; \sum_{j,k,r,s} \Lambda_{b\;ks}^{jr}\; a_k^\dagger b_s^\dagger a_j b_r \qquad , \tag{3.43}$$

where $\Lambda_{b\;ks}^{jr} = \left(\Lambda_{b\;jr}^{ks}\right)^*$. The b_r are the annihilation operators for quanta of the new species. They satisfy canonical commutation or anti-commutation relations. The ω_r are the energies of those quanta. The other symbols (ω_j, a_j and Λ_{kl}^{ij}) have the same meaning as in Eq. (3.11). As before, we quantize in a box of volume $V = L^3$ with periodic boundary conditions. The labels of the new particle states are then $r = (\vec{n}, \sigma)$, giving their momenta $\vec{p} = \frac{2\pi}{L}\vec{n}$ and their spin σ. Their energy is $\omega = \sqrt{\vec{p}\cdot\vec{p} + m_b^2}$ where m_b is the mass of the new species.

We define $c_j(t) \equiv a_j(t)e^{i\omega_j t}$ as before, and $c'_r(t) \equiv b_r(t)e^{i\omega_r t}$. The Heisenberg equations of motion for the $c'_r(t)$ are then:

$$\dot{c}'_s = -i \sum_{j,k,r} \Lambda_{b\;ks}^{jr} c_k^\dagger c_j c'_r e^{i\Omega_{jr}^{ks}\; t} \tag{3.44}$$

where $\Omega_{jr}^{ks} \equiv \omega_k + \omega_s - \omega_j - \omega_r$. Because 3-momentum is conserved in each interaction, the $\Lambda_{b\;ks}^{jr}$ have the form:

$$\Lambda_{b\;ks}^{jr} = -\lambda_{b\;ks}^{jr}\; \delta_{\vec{p}_k+\vec{p}_s,\vec{p}_j+\vec{p}_r} \quad . \tag{3.45}$$

The important contributions in the sum on the RHS of Eq. (3.44) are from terms in which both j and k label highly occupied cold axion states. Therefore

$$\dot{c}'_s \sim +i \sum_{k,j=1}^{K} \lambda_{b\;ks}^{jr} C_k^* C_j c'_r\; e^{i(\omega_s-\omega_r)t} \tag{3.46}$$

with $\vec{p}_r = \vec{p}_s + \vec{p}_k - \vec{p}_j$. As before, K is the number of highly occupied cold axion states and the C_k are defined by Eq. (3.33). Again, the sum on the RHS of Eq. (3.46) represents a random walk in complex space. The number of steps is K^2 and the typical step size is $\lambda_b\, \mathcal{N}c'$, where λ_b is the typical value of $\lambda_{b\;ks}^{jr}$. The rate at which all quanta of the new species may move to neighboring states seperated in momentum space by less than $\delta p \sim \frac{1}{\ell}$ is therefore

$$\Gamma_{b,\delta p} \sim K\mathcal{N}\lambda_b = \lambda_b\; N \tag{3.47}$$

where $N = K\mathcal{N}$ is the number of cold axions in volume V. The relaxation rate of the new species is then

$$\Gamma_b \sim \lambda_b\; N\; \frac{\delta p}{\Delta p} \sim \lambda_b\; N\; \frac{1}{\ell \Delta p} \tag{3.48}$$

where Δp is the momentum dispersion of the new species population. (If the momentum dispersion is very different in the initial state than in the final state, Δp is the larger of the two.) Eq. (3.48) assumes that the b particles are bosons or non-degenerate fermions. If they are degenerate fermions, their relaxation rate is suppressed, relative to Eq. (3.48), by Pauli blocking.

Also, let us reiterate that when most cold axions are in the lowest energy state, implying $K = 1$, thermalization is suppressed compared to the estimate in Eq. (3.48), because there is only one term in the sum of Eq. (3.46) in that case and the momentum transfer vanishes for that term.

1. *Baryons*

For non-relativistic species, such as baryons and WIMPs, the term in the Hamiltonian that describes gravitational interactions with the cold axions is

$$H_B = -G \int d^3x \; d^3x' \frac{\rho(\vec{x},t)\rho_B(\vec{x}',t)}{|\vec{x}-\vec{x}'|} \quad , \tag{3.49}$$

where

$$\rho_B(\vec{x},t) = \frac{m_B}{V} \sum_{\vec{n},\vec{n}',\sigma} b^\dagger_{\vec{n},\sigma} \; b_{\vec{n}',\sigma} \; e^{i(\vec{p}\,'-\vec{p})\cdot\vec{x}} \quad , \tag{3.50}$$

and m_B is the mass of the non-relativistic particle. This yields

$$\lambda^{\vec{n}_1,(\vec{n}_2,\sigma)}_{B\;\vec{n}_3,(\vec{n}_4,\sigma')} = +\frac{4\pi G m m_B}{V q^2} \; \delta^\sigma_{\sigma'} \quad , \tag{3.51}$$

where $\vec{q} = \vec{p}_1 - \vec{p}_3$ is the momentum transfer. Since $q \sim \ell^{-1}$, the B particles have relaxation rate

$$\Gamma_B \sim 4\pi G n m m_B \frac{\ell}{\Delta p_B} \quad , \tag{3.52}$$

where Δp_B is their momentum dispersion. Eq. (3.52) assumes that the B particles are bosons or non-degenerate fermions, as is the case for baryons and WIMPs.

2. *Hot axions*

For relativistic species, the term that describes gravitational interactions with the cold axion fluid is

$$H_r = -\int d^3x \; \frac{1}{2} h_{\alpha\beta} T^{\alpha\beta} \tag{3.53}$$

where $T^{\alpha\beta}(\vec{x},t)$ is the stress-energy-momentum tensor of this species and $h_{\alpha\beta}$ is the perturbation of the space-time metric caused by the cold axions:

$$\begin{aligned} h_{00}(\vec{x},t) &= 2G \int d^3x' \frac{\rho(\vec{x}',t)}{|\vec{x}-\vec{x}'|} \\ h_{0k}(\vec{x},t) &= 0 \\ h_{kl}(\vec{x},t) &= 2G \int d^3x' \frac{\rho(\vec{x},t)}{|\vec{x}-\vec{x}'|^3}(x_k - x'_k)(x_l - x'_l) \quad . \end{aligned} \tag{3.54}$$

Note that $h^\alpha_\alpha = 0$. For a scalar field $\phi(x)$

$$H_r = -\int d^3x \; \frac{1}{2} h_{\alpha\beta} \; \partial^\alpha\phi \; \partial^\beta\phi \quad . \tag{3.55}$$

After some algebra, Eq. (3.55) yields

$$\lambda^{\vec{n}_1,\vec{n}_2}_{r\;\vec{n}_3,\vec{n}_4} = +\frac{4\pi G m}{V q^2 \sqrt{\omega_2\omega_4}} \; [\omega_2\omega_4 + \vec{p}_2\cdot\vec{p}_4 - 2\frac{(\vec{q}\cdot\vec{p}_2)(\vec{q}\cdot\vec{p}_4)}{q^2}] \quad , \tag{3.56}$$

where $\vec{q} = \vec{p}_1 - \vec{p}_3$. The relaxation rate for relativistic scalars through gravitational interactions with the highly occupied low momentum axion modes is thus of order

$$\Gamma_r \sim 4\pi G n m \ell \quad , \tag{3.57}$$

since $q \sim \ell^{-1}$ and $\Delta p \sim \omega$.

3. Photons

The term that describes the gravitational interactions of photons with the cold axion fluid is

$$H_\gamma = -\int d^3x \frac{1}{2} h_{\alpha\beta} F^{\alpha\mu} F^{\beta}_{\ \mu} \tag{3.58}$$

where $F_{\alpha\beta}$ is the electromagnetic field strength tensor, and the $h_{\alpha\beta}$ are given by Eqs. (3.54) as before. This yields

$$\lambda^{\vec{n}_1,(\vec{n}_2,\vec{\epsilon}_2)}_{\gamma\ \ \vec{n}_3,(\vec{n}_4,\vec{\epsilon}_4)} = +\frac{8\pi G m}{V q^4 \sqrt{\omega_2 \omega_4}} \left[\omega_2\omega_4 (\vec{\epsilon}_2 \cdot \vec{q})(\vec{\epsilon}_4^{\,*} \cdot \vec{q}) + (\vec{p}_2 \times \vec{\epsilon}_2)\cdot\vec{q}\ (\vec{p}_4 \times \vec{\epsilon}_4^{\,*})\cdot\vec{q}\right] \quad , \tag{3.59}$$

where $\vec{\epsilon}_2$ and $\vec{\epsilon}_4$ are the polarization vectors of the initial and final state photons. We find therefore

$$\Gamma_\gamma \sim 4\pi G n m \ell \tag{3.60}$$

for the relaxation rate of photons. It is the same as for relativistic axions, Eq. (3.57), in order of magnitude.

IV. NUMERICAL SIMULATIONS

As far as we are aware, there has been no detailed discussion of thermalization in the condensed regime prior to this work, presumably because most many body systems thermalize in the opposite particle kinetic regime. The cold axion dark matter fluid may be the only physical system for which the condensed regime is the relevant one. Since it is impossible to observe the process of cold axion thermalization directly, we cannot verify the validity of our estimates by empirical methods. However, we may use numerical simulation as a check. In this section we construct a toy model which thermalizes in the condensed regime but is sufficiently simple that it can be simulated numerically. The simulation agrees with our estimate of its thermalization rate.

The Hamiltonian for the systems of interest to us has the general form given in Eq. (3.11) which we repeat here for convenience:

$$H = \sum_{j=1}^{M} \omega_j a_j^\dagger a_j \ + \ \sum_{i,j,k,l} \frac{1}{4}\ \Lambda^{ij}_{kl}\ a_k^\dagger a_l^\dagger a_i a_j \quad . \tag{4.1}$$

As before, let us define $c_j(t) \equiv a_j(t) e^{i\omega_j t}$. The $c_j(t)$ satisfy the Heisenberg equations of motion

$$\dot{c}_l(t) = -i \sum_{k,i,j=1}^{M} \frac{1}{2}\ \Lambda^{ij}_{kl}\ c_k^\dagger c_i c_j e^{i\Omega^{kl}_{ij} t} \quad , \tag{4.2}$$

where $\Omega^{kl}_{ij} \equiv \omega_k + \omega_l - \omega_i - \omega_j$. The system is in the condensed regime when a large number of quanta are in states whose spread $\delta\omega$ in energy is small compared to the evolution rate of the system, so that $e^{i\Omega^{kl}_{ij} t} = 1$ for the dominant terms on the RHS of Eq. (4.2). We discussed thermalization in the condensed regime in Section III.D. Our estimate for the thermalization rate is

$$\Gamma \sim \sqrt{I}\ \mathcal{N}\ \Lambda \tag{4.3}$$

where I is the number of interaction terms on the RHS of Eq. (4.2) between highly occupied states, $\mathcal{N}$ the average occupation number of those states, and Λ an average value of the Λ^{ij}_{kl}.

We may expand any state of the system

$$|\Psi(t)> = \sum_{\{\mathcal{N}\}} \Psi(\{\mathcal{N}\}, t)\ e^{-iE(\{\mathcal{N}\})t}\ |\{\mathcal{N}\}> \tag{4.4}$$

in terms of an orthonormal set of Fock space states

$$|\{\mathcal{N}\}> = |\mathcal{N}_1, \mathcal{N}_2, ..., \mathcal{N}_M> = \prod_{j=1}^{M} \frac{1}{\sqrt{\mathcal{N}_j!}} (a_j^\dagger)^{\mathcal{N}_j}\ |0> \quad . \tag{4.5}$$

These are the eigenstates of the non-interacting Hamiltonian. The corresponding eigenvalues are

$$E(\{\mathcal{N}\}) = \sum_{j=1}^{M} \mathcal{N}_j \omega_j \quad . \tag{4.6}$$

The probability for the system to be in state $|\{\mathcal{N}\}>$ at time t is $|\Psi(\{\mathcal{N}\},t)|^2$.

The time evolution equation

$$i\frac{\partial}{\partial t}|\Psi(t)>= H|\Psi(t)> \tag{4.7}$$

implies

$$i\dot{\Psi}(\{\mathcal{N}\},t) = \sum_{i,j,k,l} \frac{1}{4}\Lambda^{ij}_{kl} e^{-i\Omega^{ij}_{kl}t}\sqrt{(\mathcal{N}_i+1)(\mathcal{N}_j+1)\mathcal{N}_k\mathcal{N}_l}\ \Psi(\{^{ij}_{kl}\mathcal{N}\},t) \tag{4.8}$$

where

$$\begin{aligned} {}^{ij}_{kl}\mathcal{N}_p &= \mathcal{N}_p \qquad \text{if } p \neq i,j,k,l \\ &= \mathcal{N}_p + 1 \quad \text{if } p = i \text{ or } j \\ &= \mathcal{N}_p - 1 \quad \text{if } p = k \text{ or } l \quad . \end{aligned} \tag{4.9}$$

The $\{^{ij}_{kl}\mathcal{N}\}$ configuration is the same as the $\{\mathcal{N}\}$ configuration except that two particles are moved, from the states k and l to the states i and j. In obtaining Eqs. (4.8) and (4.9) we assumed that the couplings Λ^{ij}_{kl} vanish when $k = l$ or $i = j$. If we do not impose this restriction, Eqs. (4.8) and (4.9) are a little more complicated. However the complications do not change the estimate of the thermalization rate, so we ignore them.

The evolution of the system can be determined by solving Eqs. (4.8) numerically. For a system in the condensed regime, the important terms on the RHS of that equation all have $e^{-i\Omega^{ij}_{kl}t} = 1$, so that

$$i\dot{\Psi}(\{\mathcal{N}\},t) = \sum_{i,j,k,l} \frac{1}{4}\Lambda^{ij}_{kl}\sqrt{(\mathcal{N}_i+1)(\mathcal{N}_j+1)\mathcal{N}_k\mathcal{N}_l}\ \Psi(\{^{ij}_{kl}\mathcal{N}\},t) \quad . \tag{4.10}$$

Recall that the cold axion fluid is in the condensed regime because the axions occupy relatively few states, each state is hugely occupied ($\mathcal{N} \sim 10^{61}$), the particle states have a small spread in energy ($\delta\omega\Gamma^{-1} << 1$) yet, because $\delta\omega\ \mathcal{N}\Gamma^{-1} >> 1$, it is meaningful to ask what is the distribution of axions over the closely spaced states. The multiple requirements are satisfied only because $\mathcal{N}$ is very large. But if $\mathcal{N}$ is large, it is difficult to solve Eqs. (4.10) numerically. Indeed, the number of system states (the dimension of Hilbert space) is [30]

$$D = \frac{(N+M-1)!}{N!\ (M-1)!} \tag{4.11}$$

if N is the number of particles and M the number of particle states they occupy. Clearly, we will only be able to simulate systems with relatively small N and M. (The simulation described below has $M = 5$ and $N = 50$, hence $D = 316\ 251$ and $\mathcal{N} = 10$.) Since $\mathcal{N}$ cannot be very large in a numerical simulation, how then does one simulate a system in the condensed regime?

We may contrive a toy model in the condensed regime by setting $\Lambda^{ij}_{kl} = 0$ when $\Omega^{ij}_{kl} \neq 0$. In the example studied below, $M = 5$ and the states are equally spaced: $\omega_j = j\omega_1$ for j = 1,2, .. 5. The Λ^{ij}_{kl} all vanish except Λ^{14}_{23}, Λ^{15}_{24}, Λ^{25}_{34} and their complex conjugates Λ^{23}_{14}, Λ^{24}_{15} and Λ^{34}_{25}. The toy Hamiltonian is therefore

$$\begin{aligned} H &= \omega_1 a_1^\dagger a_1 + 2\omega_1 a_2^\dagger a_2 + 3\omega_1 a_3^\dagger a_3 + 4\omega_1 a_4^\dagger a_4 + 5\omega_1 a_5^\dagger a_5 + \Lambda^{14}_{23} a_2^\dagger a_3^\dagger a_1 a_4 + \Lambda^{14*}_{23} a_1^\dagger a_4^\dagger a_2 a_3 \\ &+ \Lambda^{15}_{24} a_2^\dagger a_4^\dagger a_1 a_5 + \Lambda^{15*}_{24} a_1^\dagger a_5^\dagger a_2 a_4 + \Lambda^{25}_{34} a_3^\dagger a_4^\dagger a_2 a_5 + \Lambda^{25*}_{34} a_2^\dagger a_5^\dagger a_3 a_4 \ . \end{aligned} \tag{4.12}$$

The toy model is a far cry from a description of the cold axion fluid but it is in the condensed regime in the sense that its evolution is governed by Eq. (4.10), and that evolution is non trivial. We may ask how quickly does the toy system reach thermal equilibrium starting from an arbitrary initial state $|\mathcal{N}_1,\mathcal{N}_2,\mathcal{N}_3,\mathcal{N}_4,\mathcal{N}_5>$. The initial state determines the energy E through Eq. (4.6). The (microcanonical ensemble) thermal averages of the $\mathcal{N}_j$ are

$$\bar{\mathcal{N}_j} = \frac{\sum_{\{\mathcal{N}\}} \mathcal{N}_j \delta(E - E(\{\mathcal{N}\}))}{\sum_{\{\mathcal{N}\}} \delta(E - E(\{\mathcal{N}\}))} \quad . \tag{4.13}$$

The $\bar{\mathcal{N}}_j$ were calculated numerically. They differ generally from the Bose-Einstein distribution

$$\bar{\mathcal{N}}_{j,\mathrm{BE}} = \frac{1}{e^{(\omega_j-\mu)/T}-1} \quad , \tag{4.14}$$

where T is temperature and μ is chemical potential, because the toy model is not in the thermodynamic limit.

We calculate the quantum mechanical averages

$$< \mathcal{N}_j(t) >= \sum_{\{\mathcal{N}\}} \mathcal{N}_j |\Psi(\{\mathcal{N}\},t)|^2 \tag{4.15}$$

as a function of time and ask how quickly do they reach the thermal averages $\bar{\mathcal{N}}_j$. Fig. 1 shows the result of a particular simulation with $N = 50$. The initial state is $|20, 5, 15, 5, 5 >$, hence $E = 120\ \omega_1$. The thermal averages for that value of E are $\{\bar{\mathcal{N}}\} = (15.25, 14.72, 9.33, 6.16, 4.53)$. The evolution was computed using Eqs. (4.10) and (4.15) with $\Lambda^{14}_{23} = \Lambda^{15}_{24} = \Lambda^{25}_{34} = 0.1$. The time step was $\Delta t = 10^{-6}$, sufficiently small that energy is conserved within 1%. Fig. 1 shows the $< \mathcal{N}_j(t) >$ as a function of t. Their values at $t = 2.3$ are $(15.57, 14.61, 9.42, 6.29, 4.59)$. There is no doubt that the system thermalizes. Eq. (4.3) estimates the thermalization rate to be $\Gamma \sim \sqrt{3} \times 10 \times 0.1 = 1.7$, i.e. the thermalization time $1/\Gamma$ is 0.6 . That estimate is consistent with the time evolution shown in Fig. 1. We ran simulations for a number of different initial conditions. In each case, the $\mathcal{N}_j(t)$ approached the appropriate thermal averages on a time scale of order $1/\Gamma \sim 0.6$.

It may appear unsurprising (and anti-climactic) that the simulations agree with the thermalization rate that we expected. Let us keep in mind, however, that there have been surprises in past simulations of thermalization. Fermi, Pasta and Ulam [33] performed a famous numerical experiment where a set of classical coupled oscillators is evolved in time according to a Hamiltonian of the form

$$H = \sum_{j=1}^{M} \left(\frac{p_j^2}{2m} + \frac{1}{2} m\omega_j^2 x_j^2 \right) + \sum_{ijkl} \Lambda_{ijkl}\ x_i x_j x_k x_l \quad . \tag{4.16}$$

They found that the system does not thermalize even after a very long time. We repeated this relatively simple simulation with $M = 10$ oscillators and also found that the system does not approach thermal equilibrium, even after a very long time. It is reassuring that, in contrast, the system of bosonic oscillators behaves in the way we expect. As far as we know, ours is the first simulation of the approach to thermal equilibrium of a set of coupled quantum oscillators.

V. AXION COSMOLOGY REVISITED

In this section, we consider how the late thermalization of axions and other species modifies the standard cosmological model. It is assumed that the estimates of the thermalization rates in Section III.D are correct. We find that cold axions may briefly thermalize after they are first produced during the QCD phase transition as a result of their $\lambda\phi^4$ self-interactions. However, this first thermalization era promptly ends and the axions are then decoupled until the photon temperature reaches approximately 500 eV. At that time the axions thermalize through their gravitational self-interactions. They form a BEC, meaning that most axions go to the lowest energy state available to them. The axion correlation length grows to sizes of order the horizon. The ratio Γ_a/H, of the cold axion thermalization rate to the Hubble rate, grows then as $a(t)^{-3}t^3$, the axions thermalize on ever shorter time scales relative to the age of the universe and the axion state tracks the lowest energy state at all times. We find that baryons enter into thermal contact with the cold axions soon after the axion correlation length has grown to be of order the horizon. It appears possible, although by no means certain, that baryons, photons and axions all reach the same temperature at about the time of equality between matter and radiation. In that case and assuming that the initial photon chemical potential is negligible, the photon temperature drops by the factor $(\frac{2}{3})^{\frac{1}{4}} = 0.9036$ compared to the standard cosmological model. We derive the implications of this for observations of cosmological parameters, specifically the baryon to photon ratio η_{BBN} at the time of primordial nucleosynthesis and the effective number N_{eff} of neutrino thermal degrees of freedom at decoupling. We consider whether neutrinos may also come into thermal contact with the cold axions, and what this would imply for η_{BBN} and N_{eff}. Finally we show that axion rethermalization by gravitational self-interactions is sufficiently fast that axions that are about to fall into a galactic gravitational potential well share their angular momenta. By almost all going to the lowest energy state for given total angular momentum, the axions acquire net overall rotation, implying $\vec{\nabla} \times \vec{v} \neq 0$ where $\vec{v}(\vec{r})$ is the velocity field of the infalling axions. In contrast, the velocity field of WIMP dark matter is irrotational. This provides a means to distinguish axions from WIMPs by observing the inner caustics of galactic halos. As mentioned in the Introduction, the evidence for caustic rings is consistent with axions and inconsistent with WIMPs.

A. QCD epoch

Cold axions are produced when the axion mass turns on during the QCD phase transition. The critical time is t_1 defined by $m(t_1)t_1 = 1$ where $m(t)$ is the axion mass. At temperatures well above 1 GeV, $m \simeq 0$ whereas at temperatures well below 100 MeV, m has its zero temperature value. A standard calculation yields [19]

$$t_1 \simeq 2 \cdot 10^{-7} \text{ sec} \left(\frac{f_a}{10^{12}\text{GeV}}\right)^{\frac{1}{3}} \quad , \quad T_1 \simeq 1 \text{ GeV} \left(\frac{10^{12}\text{GeV}}{f_a}\right)^{\frac{1}{6}} \tag{5.1}$$

where T_1 is the photon temperature at t_1. As before, f_a is the axion decay constant. How many cold axions are produced depends in part on whether inflation occurs before or after the Peccei-Quinn phase transition. If before, there are contributions to the cold axion density from vacuum realignment, string decay and wall decay. If after, the contributions from string and wall decay are absent and the contribution from vacuum realignment may be accidentally suppressed if the initial value of the homogenized axion field happens to lie close to the CP conserving minimum. The size of the string decay contribution, in case inflation occurs before the Peccei-Quinn phase transition, has been a matter of debate and controversy. There has been disagreement both on the energy spectrum of axions radiated by axion strings and on the density of axion strings in the early universe. The topic was reviewed by one of us [31]. Two more papers have appeared since then [32].

Allowing for these and other uncertainties, we write the cold axion number density at time t_1 as

$$n(t_1) = X \frac{f_a^2}{t_1} \quad . \tag{5.2}$$

X is of order two if there is no inflation after the PQ phase transition and the contribution from string decay is of the same order as that from vacuum realignment, X is of order ten if there is no inflation after the PQ phase transition and the contribution from string decay dominates over that from vacuum realignment(the contribution from wall decay is thought to be subdominant always), and X is of order one half the square of the sine of the misalignment angle if there is inflation after the PQ phase transition. The misalignment angle is a random number, between 0 and 2π, which has the same value in our whole visible universe in this case.

After t_1 the number of axions is conserved in the sense that all axion number changing processes, such as axion decay to two photons, happen on time scales vastly longer than the age of the universe. Eqs. (5.1) and (5.2) imply then the cold axion number density as a function of time

$$n(t) \simeq \frac{4 \cdot 10^{47}}{\text{cm}^3} X \left(\frac{f_a}{10^{12}\text{GeV}}\right)^{\frac{5}{3}} \left(\frac{a(t_1)}{a(t)}\right)^3 \quad . \tag{5.3}$$

Most of the cold axions are non-relativistic shortly after t_1 because the axion momenta are of order $\frac{1}{t_1}$ at time t_1 and vary with time as $a(t)^{-1}$. Hence we may obtain the axion energy density today [19, 31]

$$\Omega_a \equiv \frac{8\pi G}{3H_0^2} m n(t_0) \simeq 0.3 \; X \left(\frac{f_a}{10^{12}\text{GeV}}\right)^{\frac{7}{6}} \quad . \tag{5.4}$$

The velocity dispersion of cold axions is

$$\delta v(t) \sim \frac{1}{m t_1} \frac{a(t_1)}{a(t)} \tag{5.5}$$

if each axion remains in whatever state it is in, i.e. if axion interactions are negligible. We refer to this case as the limit of decoupled cold axions (see subsection II.C.1). If decoupled, the average state occupation number of the cold axions is [2]

$$\mathcal{N} \sim n \frac{(2\pi)^3}{\frac{4\pi}{3}(m\delta v)^3} \sim 10^{61} \; X \left(\frac{f_a}{10^{12}\text{GeV}}\right)^{\frac{8}{3}} \quad . \tag{5.6}$$

Because $\mathcal{N}$ is huge, we may expect cold axions to form a Bose-Einstein condensate. Their energy dispersion $\delta\omega = \frac{1}{2}m(\delta v)^2$ is much smaller than the critical temperature

$$T_c(t) = \left(\frac{\pi^2 n(t)}{\zeta(3)}\right)^{\frac{1}{3}} \simeq 300 \text{ GeV } X^{\frac{1}{3}} \left(\frac{f_a}{10^{12}\text{GeV}}\right)^{\frac{5}{9}} \frac{a(t_1)}{a(t)} \tag{5.7}$$

for BEC. Note that the critical temperature is calculated using the relativistic Bose-Einstein distribution since, for the axion densities envisaged, the critical temperature is much larger than the axion mass.

Actually, there are four conditions for a gas to form a Bose-Einstein condensate: 1) the particles are identical bosons, 2) their number is conserved, 3) their phase space density in units of $h^{-3} = (2\pi\hbar)^{-3}$ is of order one or larger (equivalently their average quantum state occupation number $\mathcal{N}$ is of order one or larger), and 4) the particles are in thermal equilibrium. The first three conditions are clearly satisfied in the case of cold axions. The fourth condition is the critical one since it is not obviously satisfied. Indeed, axions are thought to be very weakly interacting.

Axions are in thermal equilibrium if their relaxation rate Γ_a is large compared to the Hubble expansion rate H. We noted in Section III that the formula for the relaxation rate differs whether the particles in the fluid are in the 'particle kinetic' regime or in the 'condensed' regime. To see whether the axions thermalize by $\lambda\phi^4$ self-interactions, we use Eqs. (3.25) and (3.29) in the particle kinetic regime, and Eq. (3.38) in the condensed regime. At t_1 both estimates give the same answer [2], namely:

$$\Gamma_\lambda(t_1) \sim H(t_1) \tag{5.8}$$

indicating that the axions barely thermalize at time t_1 by $\lambda\phi^4$ self-interactions. That the two estimates agree with one another follows from the fact that

$$\delta\omega(t_1) = \frac{1}{2}m(t_1)(\delta v(t_1))^2 \sim \frac{1}{2m(t_1)t_1^2} = H(t_1) \quad . \tag{5.9}$$

Since $\Gamma_\lambda(t_1) \sim \delta\omega(t_1)$, thermalization of cold axions by $\lambda\phi^4$ interactions is, at time t_1, at the borderline between the particle kinetic and condensed regimes. We had noted earlier that at the boundary between the two regimes, the two estimates of the relaxation rate always agree with one another; see Eq. (3.41).

After t_1 we must use Eq. (3.38) since we are in the condensed regime then. It informs us that $\Gamma_\lambda(t)/H(t) \propto a(t)^{-3}t \propto t^{-\frac{1}{2}}$, i.e. that even if axions thermalize at time t_1 they stop doing so shortly thereafter. Nothing much changes as a result of this brief epoch of thermalization since in either case, whether it occurs or not, the correlation length $\ell(t) \sim t_1 a(t)/a(t_1)$.

To see whether gravitational interactions cause the cold axions to form a BEC, we use Eq. (3.40). It implies

$$\Gamma_g(t)/H(t) \sim 8\pi G n m^2 \ell^2 t \sim 5 \cdot 10^{-7}\ \frac{a(t_1)}{a(t)}\frac{t}{t_1} X \left(\frac{f_a}{10^{12}\text{GeV}}\right)^{\frac{2}{3}} \tag{5.10}$$

once the axion mass has reached its zero temperature value, shortly after t_1. Gravitational self-interactions are too slow to cause thermalization of cold axions near the QCD phase transition but, because $\Gamma_g/H \propto a^{-1}(t)t \propto a(t)$, they do cause the cold axions to thermalize later on [2].

B. Axion BEC formation

The RHS of Eq. (5.10) reaches one at a time t_{BEC} when the photon temperature is of order

$$T_{\text{BEC}} \sim 500\text{ eV } X \left(\frac{f_a}{10^{12}\text{ GeV}}\right)^{\frac{1}{2}} \quad . \tag{5.11}$$

The axions thermalize then and form a BEC as a result of their gravitational self-interactions. The whole idea may seem far-fetched because we are used to think that gravitational interactions among particles are negligible. The axion case is special, however, because almost all particles are in a small number of states with very long de Broglie wavelength, and gravity is long range. By gravitational self-interactions the axions modify their momentum distribution till their entropy is maximized for the available energy, which in this case means that they form a BEC.

Axion BEC causes the correlation length to increase. Indeed in an infinite volume, when all particles are in the lowest energy state, the momentum dispersion is theoretically zero and the correlation length infinite. This ideal state never occurs because thermalization and hence BEC formation are constrained by causality. The axions in one horizon are unaware of the doings of axions in the next horizon. Hence we expect the correlation length ℓ, which may now be thought of as the size of condensate patches, to become of order but less than the horizon. The growth in the correlation length causes the thermalization to accelerate; see Eq. (5.10). Once l is some fraction of t, $\Gamma_g(t)/H(t) \propto a(t)^{-3}t^3$, implying that thermalization occurs on ever shorter time scales compared to the Hubble time.

C. Thermal contact with other species

The rate at which non-relativistic species such as baryons change their momentum distribution through gravitational interactions with the cold axion fuid is given by Eq. (3.52). The momentum dispersion of baryons is of order $\Delta p \sim \sqrt{3m_B T}$ where T is the photon temperature. We will assume here that cold axions are the bulk of the dark matter. The Friedmann equation implies then

$$4\pi G n m \sim \frac{3}{8t^2}\left(\frac{t}{t_{\rm eq}}\right)^{\frac{1}{2}} \tag{5.12}$$

for $t < t_{\rm eq}$, where $t_{\rm eq}$ is the time of equality between matter and radiation. Hence

$$\Gamma_B/H \sim \frac{1}{4}\frac{\ell}{\sqrt{t t_{\rm eq}}}\sqrt{\frac{3m_B}{T}} \sim \frac{\ell}{t}\left(\frac{t}{t_{\rm BEC}}\right)^{\frac{3}{4}}\left(\frac{500\ {\rm eV}}{T_{\rm BEC}}\right)^{\frac{3}{2}} \quad . \tag{5.13}$$

Eq. (5.13) shows that baryons reach thermal contact with the axion BEC when ℓ becomes of order t or soon after that.

Photons are in thermal contact with the baryons, but the nature and degree of this thermal contact are changing at the time of axion BEC formation [34]. Baryons interact with electrons by Coulomb scattering. Electrons interact with photons by Compton scattering, double Compton scattering and bremsstrahlung. Above approximately 1 keV photon temperature, double Compton scattering and bremsstrahlung assure chemical equilibrium between baryons and photons (the number of photons is not conserved in these processes). Below approximately 1 keV photon temperature, Compton scattering is the only important interaction remaining. It maintains kinetic, but not chemical, equilibrium between baryons and photons till approximately 100 eV photon temperature. Below 100 eV, the degree of kinetic equilibrium progressively diminishes till approximately 2 eV, when it disappears altogether.

In any case, as long as there is only thermal contact between baryons and a few low momentum modes of the axion field, only a very small amount of energy can be exchanged between the axion field and the other species. However, as time goes on, higher and higher momentum modes of the axion field reach thermal contact with its highly occupied low momentum modes. Eq. (3.57) gives the relaxation rate Γ_r of the axion field as a whole, including relativistic states. The relaxation rate of photons Γ_γ, Eq. (3.60), is of the same order of magnitude. Combining Eqs. (3.57) and (3.60) with the Friedmann equation, we have

$$\Gamma_\gamma/H \sim \Gamma_r/H \sim \frac{3}{2} H\ell\ \frac{\rho_a}{\rho_{\rm tot}} \quad , \tag{5.14}$$

where ρ_a is the cold axion density and $\rho_{\rm tot}$ the total density. Since $\ell \propto t$, Eq. (5.14) implies that Γ_γ/H and Γ_r/H grow proportionally to $a(t)$ till equality and remain constant after that. The critical parameter is their value at equality

$$\Gamma_\gamma/H|_{t_{\rm eq}} \sim \Gamma_r/H|_{t_{\rm eq}} \sim \frac{\ell(t_{\rm eq})}{t_{\rm eq}} \quad . \tag{5.15}$$

Thermal contact between axions and photons is established if the RHS of Eq. (5.15) is of order one, i.e. if the axion correlation length is horizon size at equality. To show that the axion BEC correlation length becomes truly as large as the horizon is a problem, involving both out-of-equilibrium statistical mechanics and general relativity, which we do not know how to solve at present.

Hence we consider at this stage two possibilities, which we call cases A and B. In case A, $\Gamma_{r,\gamma}/H$ do not reach one before equality (because ℓ, although proportional to t, may be much less than t, e.g. $\ell = t/100$), and hence thermal contact gets established only between baryons and low momentum modes of the axion field. In case B, $\Gamma_{r,\gamma}/H$ do reach one before equality and thermal equilibrium is reached between baryons, axions and photons. This equilibrium is kinetic only since gravitational interactions conserve particle number for all the species involved.

We should ask whether neutrinos may also reach thermal contact with the highly occupied low momentum axion modes, in which case neutrinos, axions, baryons and photons would all reach the same temperature. We believe this possibility, which we call case C, unlikely for the following reason. Eq. (3.42) does not apply to degenerate fermions because of Pauli blocking. Cosmic neutrinos are semi-degenerate since they have a thermal distribution with zero chemical potential. Because of partial Pauli blocking, their thermalization is slower than that of relativistic axions, Eq. (3.57). Since relativistic axions only barely reach thermal contact with the highly occupied low momentum modes of the axion field if they do so at all, and thermal contact between those low momentum modes of the axion field and neutrinos is delayed relative to relativistic axions, it appears most likely that neutrinos remain decoupled from the axions at all times. Although we believe case C unlikely, we consider its implications below along with the other two cases.

D. Implications for cosmological parameters

In case A, the baryons reach the same temperature as the low momentum states of the axion field but only a very small amount of energy is transferred from baryons to axions, because the relativistic states of the axion field remain decoupled from its low momentum states. The cosmological parameters are the same as in the standard cosmological model with WIMP dark matter.

In case B, baryons, axions and photons all reach the same temperature. The axions are heated whereas the photons are cooled. The number of photons is unchanged implying that their chemical potential stays at zero or, if photons have a small negative chemical potential to start with, increases till it reaches zero. There is photon Bose-Einstein condensation, i.e. the excess photons condense into the lowest energy available state, which is a plasma wave with vanishing wavevector. With zero chemical potential, the photon energy spectrum is Planckian, as required by observation. Energy conservation implies

$$\rho_{\gamma i} = \frac{\pi^2}{15} T_{\gamma i}^4 = \rho_{\gamma f} + \rho_{af} = \frac{\pi^2}{30} T_{\gamma_f}^4 (2+1) \quad . \tag{5.16}$$

Hence $T_{\gamma f} = \left(\frac{2}{3}\right)^{\frac{1}{4}} T_{\gamma i} = 0.9036\ T_{\gamma i}$ in case B. In Eq. (5.16), we neglected tiny contributions from the kinetic energy density of the initial state axions (of order $\frac{1}{2} mn(\delta v)^2 \sim \rho_a (\frac{1}{mt_1} \frac{T_{\rm eq}}{T_1})^2 \sim 10^{-24} \rho_a$ near equality), the kinetic energy density of the baryons (of order the baryon to photon ratio, or $\sim 10^{-9}$, relative to the photon energy density) and the energy density of the condensed photons in the final state (of order $\frac{\omega_{\rm pl}}{T_\gamma} \sim 10^{-9}$ relative to the photon energy density at equality, where $\omega_{\rm pl}$ is the plasma frequency). We also assumed that the initial chemical potential of the photons is zero. Finally, we ignored the fact that, while the transfer of energy between photons and axions takes place, the expansion of the universe affects photons and axions differently because axions have mass. The corresponding error is of order $m/T_{\rm eq} \sim 10^{-5}$, or less.

After the axions have been heated by thermal contact with the photons, the fraction of axions in thermally excited states is of order

$$\left(\frac{T_{\rm eq}}{T_c(t_{\rm eq})}\right)^3 \sim 4 \cdot 10^{-8}\ \frac{1}{X}\ \left(\frac{10^{12}\ {\rm GeV}}{f_a}\right)^{\frac{13}{6}} \quad . \tag{5.17}$$

All others are condensed in the lowest energy available state. The condensed axions are cold dark matter, with the special properties that are the topic of this paper. The axions in thermally excited states contribute one bosonic degree of freedom to radiation, and are a form of hot dark matter. The possibility that the same particle may contribute cold and hot dark matter components was recently discussed [35]. After axions, baryons and photons have all reached the same temperature, further thermalization is suppressed because, once most of the axions are in the same state, the only interactions that are enhanced by large occupation numbers are interactions without momentum transfer (see Section III.D).

In case B, cosmological parameters are modified compared to their values in the standard model with WIMP dark matter. Since the photons cool between the epoch of primordial nucleosynthesis (BBN, for short) and decoupling, and their temperature at decoupling is known, their temperature at BBN is larger by the factor $\left(\frac{3}{2}\right)^{\frac{1}{4}}$ compared to the standard model. Because baryon number is conserved, the baryon to photon ratio $\eta \equiv n_b/n_\gamma$is smaller at BBN than at decoupling. The baryon to photon ratio at decoupling is reliably determined from measurements of the anisotropy spectrum of the cosmic microwave radiation. The latest WMAP result [36] is $\eta_{\rm dec} = (6.190 \pm 0.145)\ 10^{-10}$. Since the photon number density $n_\gamma \propto T^3$, the value of η at BBN is

$$\eta_{\rm BBN} = \left(\frac{2}{3}\right)^{\frac{3}{4}} \eta_{\rm dec} = (4.57 \pm 0.11)\ 10^{-10} \tag{5.18}$$

in case B, whereas $\eta_{\rm BBN} = \eta_{\rm dec}$ in the standard model. Under the assumption that there are three neutrino species, $\eta_{\rm BBN}$ is the main parameter controlling the primordial abundances of the light elements. In the standard model, there is generally good agreement between the observed and predicted abundances of three light elements (D, ^{4}He, ^{3}He) but there is a discrepancy for ^{7}Li, the so-called 'Lithium problem' [37]. The Lithium problem is alleviated in case B, and perhaps solved altogether, because of the lower value of $\eta_{\rm BBN}$ [12]. On the other hand, the agreement that occurs in the standard model between the observed and predicted abundance of deuterium is spoiled [12]. The ^{3}He abundance [37] is not measured sufficiently precisely to distinguish between the standard model and case B [12]. Finally, the observed abundance of ^{4}He has changed so much recently [38] compared to its accepted value a few years ago [39] that it is unclear for the time being how that information should be used.

Case B differs also from the standard cosmological model in that it has more radiation in collisionless species (axions and neutrinos). The radiation content of the universe is commonly given in terms of the effective number $N_{\rm eff}$ of thermally excited neutrino degrees of freedom, defined by

$$\rho_{\rm rad} = \rho_\gamma \left[1 + N_{\rm eff}\ \frac{7}{8}\left(\frac{4}{11}\right)^{\frac{4}{3}}\right] \tag{5.19}$$

where $\rho_{\rm rad}$ is the total energy density in radiation (including photons, neutrinos and axions) and ρ_γ is the energy density in photons only. The standard model predicts $N_{\rm eff} = 3.046$, slightly larger than 3 because the three neutrinos heat up a little during e^+e^- annihilation. In case B

$$\rho_{\rm rad} = \rho_\gamma + \rho_a + \rho_\nu = \rho_\gamma \left[1 + \frac{1}{2} + (3.046)\frac{7}{8}\left(\frac{4}{11}\right)^{\frac{4}{3}}\frac{3}{2}\right] \tag{5.20}$$

taking account of the fact that not only is there an extra species of radiation (axions) but also the contribution of neutrinos is boosted because the photons have cooled relative to them. Eq. (5.20) implies $N_{\rm eff} = 6.77$. At present, most measurements place $N_{\rm eff}$ between 4 and 5, with one σ uncertainties of order 1 [36, 40]. The tendency for the measured values to be larger than 3.046 has been taken sufficiently seriously to prompt proposals for new physics involving extra neutrino species or a neutrino asymmetry [41]. The Planck mission is expected to measure $N_{\rm eff}$ with much greater precision [42]. In so doing, it may shed light on the nature of dark matter.

In case C, the cosmological parameters differ from their standard values even more than in case B. Energy conservation implies in case C

$$\begin{aligned}\rho_{\gamma i} + \rho_{\nu i} &= \frac{\pi^2}{30}T_{\gamma i}^4\left[2 + (3.046)\cdot 2\cdot\frac{7}{8}\left(\frac{4}{11}\right)^{\frac{4}{3}}\right] \\ &= \rho_{\gamma f} + \rho_{af} + \rho_{\nu f} = \frac{\pi^2}{30}T_f^4(2+1) + \rho_{\nu f}(T_f, \mu_{\nu f})\end{aligned} \tag{5.21}$$

where T_f is the common final temperature of photons, axions and neutrinos, and $\mu_{\nu f}$ is the final chemical potential of the neutrinos. In writing Eq. (5.21) we make the same approximations as for Eq. (5.16). When gravitational interactions establish kinetic equilibrium between axions, photons and neutrinos, the photons cool whereas the axions and neutrinos heat up. Since the number of neutrinos is conserved in this process, the neutrinos acquire a negative chemical potential. To obtain T_f we solve numerically

$$n_{\nu i} = \frac{3\zeta(3)}{4\pi^2}T_{\nu i}^3 = n_{\nu f} = \int \frac{d^3k}{(2\pi)^3}\frac{1}{e^{\frac{(k-\mu_{\nu f})}{T_f}} + 1} \tag{5.22}$$

with $T_{\nu i} = \left(\frac{4}{11}\right)^{\frac{1}{3}} T_{\gamma i}$, and Eq. (5.21) with

$$\rho_{\nu f} = 2(3.046)\int \frac{d^3k}{(2\pi)^3}\frac{k}{e^{\frac{(k-\mu_{\nu f})}{T_f}} + 1} \quad . \tag{5.23}$$

This yields $T_f = 0.873 T_{\gamma i}$ and $\mu_{\nu f} = -0.65 T_f$. The photons cool even more than in case B ($T_f = 0.904 T_{\gamma i}$) because their heat is transferred to neutrinos as well as axions. In case C, the baryon to photon ratio at the epoch or primordial nucleosynthesis is

$$\eta_{\rm BBN} = (0.873)^3\eta_{\rm dec} = (4.12 \pm 0.10)10^{-10} \tag{5.24}$$

using again the WMAP value $\eta_{\rm dec} = (6.190 \pm 0.145)10^{-10}$. The total radiation density is also higher. Equating the RHS of Eq. (5.21) with the RHS of Eq. (5.19) yields $N_{\rm eff} = 8.3$.

E. Tidal torquing with axion BEC

Let us consider a region of size L inside of which the axion state (i.e. the state that most axions are in) stops being the lowest energy available state because the background is time dependent. Under what conditions is thermalization by gravitational self-interactions sufficiently fast that the condensed axions remain in the lowest energy state as the

background evolves? We use the same heuristic reasoning that led us to Eq. (3.42), which we later verified by more formal derivations in a number of cases in Section III.E. We expect that the axion BEC rethermalizes provided the gravitational forces produced by the BEC are larger than the typical rate $\dot{p}$ of change of axion momenta required for the axions to remain in the lowest energy state. The gravitational forces are of order $4\pi G n m^2 \ell$. In this case, the correlation length ℓ must be taken to be of order the size L of the region of interest since the gravitational fields due to axion BEC outside the region do not help the thermalization of the axions within the region. Hence the condition is

$$4\pi G n m^2 L \gtrsim \dot{p} \quad . \tag{5.25}$$

We now apply this criterion to the question whether axions rethermalize sufficiently quickly that they share angular momentum when they are about to fall into a galactic gravitational potential well.

We use the self-similar infall model of galactic halo formation to estimate L and $\dot{p}$. L is of order a few times the turnaround radius $R(t)$, say $L(t) \sim 3R(t)$, whereas $p(t) \sim m v_{\rm rot}(t) j_{\rm max}$ where $v_{\rm rot}$ is the rotation velocity and $j_{\rm max}$ is the dimensionless number characterizing the amount of angular momentum of the halo. In the self-similar model, $v_{\rm rot}(t) \sim R(t)/t$ and $R(t) \propto t^{\frac{2}{3}+\frac{2}{9\epsilon}}$ where ϵ is in the range 0.25 to 0.35 [7]. Assuming that most of the dark matter is axions, the Friedmann equation implies

$$4\pi G n m = \frac{3}{2} H(t)^2 = \frac{2}{3t^2} \tag{5.26}$$

for $t > t_{\rm eq}$. The LHS of Eq. (5.25) is therefore of order

$$2m\frac{R(t)}{t^2} \sim 2m v_{\rm rot}(t)\frac{1}{t} \tag{5.27}$$

whereas its RHS is of order

$$\frac{d}{dt}\left[m j_{\rm max} v_{\rm rot}(t_0)\left(\frac{t}{t_0}\right)^{-\frac{1}{3}+\frac{2}{9\epsilon}}\right] = m j_{\rm max} v_{\rm rot}(t)\frac{1}{t}\left(\frac{2}{9\epsilon}-\frac{1}{3}\right) \quad . \tag{5.28}$$

The typical value of $j_{\rm max}$ is 0.18 . Hence Eq. (5.25) is satisfied at all times from equality till today by a margin of order $\frac{2}{j_{\rm max}(\frac{2}{9\epsilon}-\frac{1}{3})} \sim 30$.

We conclude that the axion BEC does rethermalize before falling into the gravitational potential well of a galaxy. Most axions go to the lowest energy state consistent with the total angular momentum acquired from neighboring inhomogeneities through tidal torquing [43]. That state is a state of rigid rotation on the turnaround sphere, implying $\vec{\nabla} \times \vec{v} \neq 0$ where $\vec{v}$ is the velocity field of the infalling axions. In contrast, the velocity field of ordinary cold dark matter is irrotational. The inner caustics of galactic halos are different in the two cases. Axions produce caustic rings whereas ordinary cold dark matter produces the 'tent-like' caustics described in Ref. [5]. There is evidence for the existence of caustic rings in various galaxies at the radii predicted by the self-similar infall model. For a review of this evidence see Ref. [8]. It is shown in Ref. [9] that the phase space structure of galactic halos implied by the evidence for caustic rings is precisely and in all respects that predicted by the assumption that the dark matter is a rethermalizing BEC.

VI. SUMMARY

The purpose of this paper was to investigate when and to what extent cold axions differ from ordinary cold dark matter, such as WIMPs and sterile neutrinos.

In Section II, we showed that cold axions behave as ordinary cold dark matter on all scales of observational interest when they are decoupled. Observable differences between cold axions and ordinary cold dark matter occur only when the axions self-interact. When the axions self-interact at a sufficiently high rate, they thermalize and form a Bose-Einstein condensate. Before that time, the axions are described by a free classical field and are indistinguishable from ordinary cold dark matter on all scales of observational interest. After Bose-Einstein condensation, almost all axions are in the same state. If that state is time independent, axions again behave as ordinary cold dark matter on all scales of observational interest. Observable differences occur if and only if the axions rethermalize so that the axion state tracks the lowest energy state.

In Section III, we calculated the thermalization rates of cold axions through $\lambda\phi^4$-type self-interactions and through gravitational self-interactions. We described the axion field as a set of coupled quantum-mechanical oscillators and

asked how quickly such a set of oscillators approaches thermal equilibrium. We found that there are two distinct regimes: the 'particle kinetic regime' defined by the condition that the energy dispersion is large compared to the interaction rate ($\delta\omega >> \Gamma$), and the opposite 'condensed regime' where $\delta\omega << \Gamma$. We derived the Boltzmann equation as an operator statement in the particle kinetic regime. However, cold axion thermalization occurs almost entirely in the condensed regime. We derived estimates for the thermalization rate in the condensed regime, and applied the estimates to cold axions and to other species (baryons, photons and relativistic axions) that may come into thermal contact with the cold axions.

In Section IV, we performed numerical simulations to check our estimates of thermalization rates in the condensed regime. We constructed a toy model with 50 quanta distributed among 5 oscillators. The exact quantum-mechanical evolution of the toy model was solved numerically for a variety of initial conditions. It was found that the toy system thermalizes and does so on the time scale predicted by the analytical estimate in Section III.

In Section V, we investigated what changes the thermalization of cold axions brings to axion cosmology. It was found that cold axions thermalize by gravitational self-interactions when the photon temperature is of order 500 eV. When they thermalize, the cold axions form a Bose-Einstein condensate. The axion correlation length grows to a size of order but smaller than the horizon. Shortly thereafter, baryons come into thermal contact with the axions. As time goes on, increasingly higher momentum modes of both the axion field and the photon field come into thermal contact with the cold axions. It is possible, but by no means certain, that full thermal equilibrium is established among axions, photons and baryons. This would imply a drop in the photon temperature by the factor $\left(\frac{2}{3}\right)^{\frac{1}{4}} = 0.9036$, at about the time of equality between matter and radiation. We derived the implications of this for cosmological parameters, specifically the baryon to photon ratio at the time of primordial nucleosynthesis and the effective number of neutrinos (a measure of the radiation content of the universe) at the time of decoupling. Finally we showed that cold axions thermalize sufficiently fast by gravitational self-interactions that the axions about to fall into a galactic gravitational well acquire a state of net overall rotation. In contrast, ordinary cold dark matter falls in with an irrotational velocity field. The inner caustics of the galactic halo are different in the two cases. The occurrence of caustic rings of dark matter in galactic halos is inconsistent with ordinary cold dark matter, but consistent with axion BEC.

Acknowledgments

We have benefitted from conversations with many colleagues. In particular, we would like to thank Georg Raffelt, Lawrence Widrow, Edward Witten, Jorge Gamboa, Francisco Mendez, Sergei Obukhov, David Lyth, Charles Thorn, Charles Sommerfield, Richard Woodard, Leslie Rosenberg and Gary Steigman. We are grateful to the UF HPC Center for computer time. P.S. would like to thank the CERN Theory Group and the organizers of the DMUH11 workshop for their support and hospitality while working on this paper. This work was supported in part by the U.S. Department of Energy under grant DE-FG02-97ER41209.

[1] Reviews include: *Particle Dark Matter* edited by Gianfranco Bertone, Cambridge University Press 2010; E.W. Kolb and M. Turner, *The Early Universe*, Addison Wesley 1990.
[2] P. Sikivie and Q. Yang, Phys. Rev. Lett. 103 (2009) 111301.
[3] P. Sikivie, Phys. Lett. B432 (1998) 139.
[4] P. Sikivie, Phys. Rev. D60 (1999) 063501.
[5] A. Natarajan and P. Sikivie, Phys. Rev. D73 (2006) 023510.
[6] J.A. Fillmore and P. Goldreich, Ap. J. 281 (1984) 1; E. Bertschinger, Ap. J. Suppl. 58 (1985) 39.
[7] P. Sikivie, I. Tkachev and Y. Wang, Phys. Rev. Lett. 75 (1995) 2911; Phys. Rev. D56 (1997) 1863.
[8] L. Duffy and P. Sikivie, Phys. Rev. D78 (2008) 063508.
[9] P. Sikivie, Phys. Lett. B 695 (2011) 22.
[10] B. Moore, in the Proceedings of the 3d International Workshop on the Identification of Dark Matter (York, September 2000), edited by N. Spooner and V. Kudryatsev, World Scientific, p 93; A. Helmi, S.D.M. White and V. Springel, MNRAS 339 (2003) 834; J. Diemand and M. Kuhlen, Ap. J. 680 (2008) L25; M. Vogelsberger, S.D.M. White, R. Mohayaee and V. Springel, MNRAS 400 (2009) 2174; M. Vogelsberger and S.D.M. White, MNRAS 413 (2011) 1419.
[11] A. Natarajan and P. Sikivie, Phys. Rev. D72 (2005) 083513.
[12] O. Erken, P. Sikivie, H. Tam and Q. Yang, Phys. Rev. Lett. 108 (2012) 061304.
[13] S. Dodelson, *Modern Cosmology*, Academic Press 2003.
[14] P. Sikivie and J. Ipser, Phys. Lett. B291 (1992) 288.
[15] P. McDonald et al., Ap. J. 543 (2000) 1; R. Croft et al., Ap. J. 581 (2002) 20; U. Seljak, A. Makharov, P. McDonald and H. Trac, Phys. Rev. Lett. 97 (2006) 191303.
[16] C. Schmid, D.J. Schwarz and P. Widerin, Phys. Rev. D59 (1999) 043517; C. Boehm, P. Fayet and R. Schaeffer, Phys. Lett. B518 (2001) 8; X. Chen, M. Kamionkowski and X. Zhang, Phys. Rev. D64 (2001) 021302; S. Hofmann, D. Schwarz and H. Stöcker, Phys. Rev. D64 (2001) 083507.
[17] S. Dodelson and L.M. Widrow, Phys. Rev. Lett. 72 (1994) 17; X.-D. Shi and G.M. Fuller, Phys. Rev. Lett. 82 (1999) 2832; T. Asaka, S. Blanchet and M. Shaposhnikov, Phys. Lett. B631 (2005) 151; A. Boyarsky, J. Lesgourgues, O. Ruchayskiy and M. Viel, Phys. Rev. Lett. 102 (2009) 201304, and references therein.
[18] C.J. Pethik and H. Smith, *Bose-Einstein Condensation in Dilute Gases*, Cambridge University Press 2002.
[19] J. Preskill, M. Wise and F. Wilczek, Phys. Lett. B120 (1983) 127; L. Abbott and P. Sikivie, Phys. Lett. B120 (1983) 133; M. Dine and W. Fischler, Phys. Lett. B120 (1983) 137.
[20] J. Ipser and P. Sikivie, Phys. Rev. Lett. 50 (1983) 925.
[21] M. Bianchi, D. Grasso and R. Ruffini, Astron. Astrophys. 231 (1990) 301.
[22] J. Hwang and H. Noh, Phys. Lett. B680 (2009) 1.
[23] N. Kaiser and L. Widrow, Ap. J. 416 (1993) L71; P. Coles and K. Spencer, MNRAS 342 (2003) 176.
[24] S.-J. Sin, Phys. Rev. D50 (1994) 3650; J. Goodman, New Astronomy Reviews 5 (2000) 103; W. Hu, R. Barkana and A. Gruzinov, Phys. Rev. Lett. 85 (2000) 1158; E.W. Mielke and J.A. Vélez Pérez, Phys. Lett. B671 (2009) 174; J.-W. Lee and S. Lim, JCAP 1001 (2010) 007; A. Lundgren, M. Bondarescu, R. Bondarescu and J. Balakrishna, Ap. J. 715 (2010) L35; D.J. Marsh and P.G. Ferreira, Phys. Rev. D82 (2010) 103528; V. Lora et al., arXiv:1110.2684.
[25] R.D. Peccei and H. Quinn, Phys. Rev. Lett. 38 (1977) 1440 and Phys. Rev. D16 (1977) 1791.
[26] S. Weinberg, Phys. Rev. Lett. 40 (1978) 223.
[27] F. Wilczek, Phys. Rev. Lett. 40 (1978) 279.
[28] D.V. Semikoz and I.I. Tkachev, Phys. Rev. D55 (1997) 489.
[29] G. Baym and L.P. Kadanoff, *Quantum Statistical Mechanics*, Benjamin 1962.
[30] K. Huang, *Statistical Mechanics*, Wiley 1987.
[31] P. Sikivie, Lect. Notes Phys. 741 (2008) 19.
[32] O. Wantz, E.P.S. Shellard, Phys. Rev. D82, 123508 (2010); T. Hiramatsu et al., arXiv:1012.5502.
[33] E. Fermi, J. Pasta and S. Ulam, *Studies of Nonlinear Problems*, Document LA-1940 (May 1955); G.P. Berman and F.M. Israilev, Chaos 15 (2001).
[34] W. Hu and J. Silk, Phys. Rev. D48 (1993) 485; W. Hu, Ph.D. Thesis, 1995.
[35] I. Rodriguez-Montoya et al., arXiv:1110.2751.
[36] E. Komatsu et al., Ap.J. Suppl. 192 (2011) 18.
[37] G. Steigman, Int. J. Mod. Phys. E 15 (2006) 1; F. Iocco et al., Phys. Rep. 472 (2009) 1; R.H. Cyburt, B.D. Fields, K.A. Olive, JCAP 0811 (2008) 012.
[38] Y.I. Izotov, T.X. Thuan and G. Stasińska, Ap. J. 662 (2007) 15; Y.I. Izotov and T.X. Thuan, Ap. J. 710 (2010) L67.
[39] V. Luridiana et al., Ap. J. 592 (2003) 846.
[40] J. Hamann et al., JCAP **07** (2010) 022; J. Dunkley et al., Ap. J. 739 (2011) 52; R. Keisler et al., arXiv:1105.3182.
[41] L.M. Krauss, C. Lunardini, C. Smith, arXiv:1009.4666; J. Hamann et al., Phys. Rev. Lett. **105** (2010) 181301.
[42] K. Ichikawa, T. Sekiguchi, T. Takahashi, Phys. Rev. **D78** (2008) 083526.
[43] P.J.E. Peebles, Ap. J. 155 (1969) 2, and Astron. Ap. 11 (1971) 377.

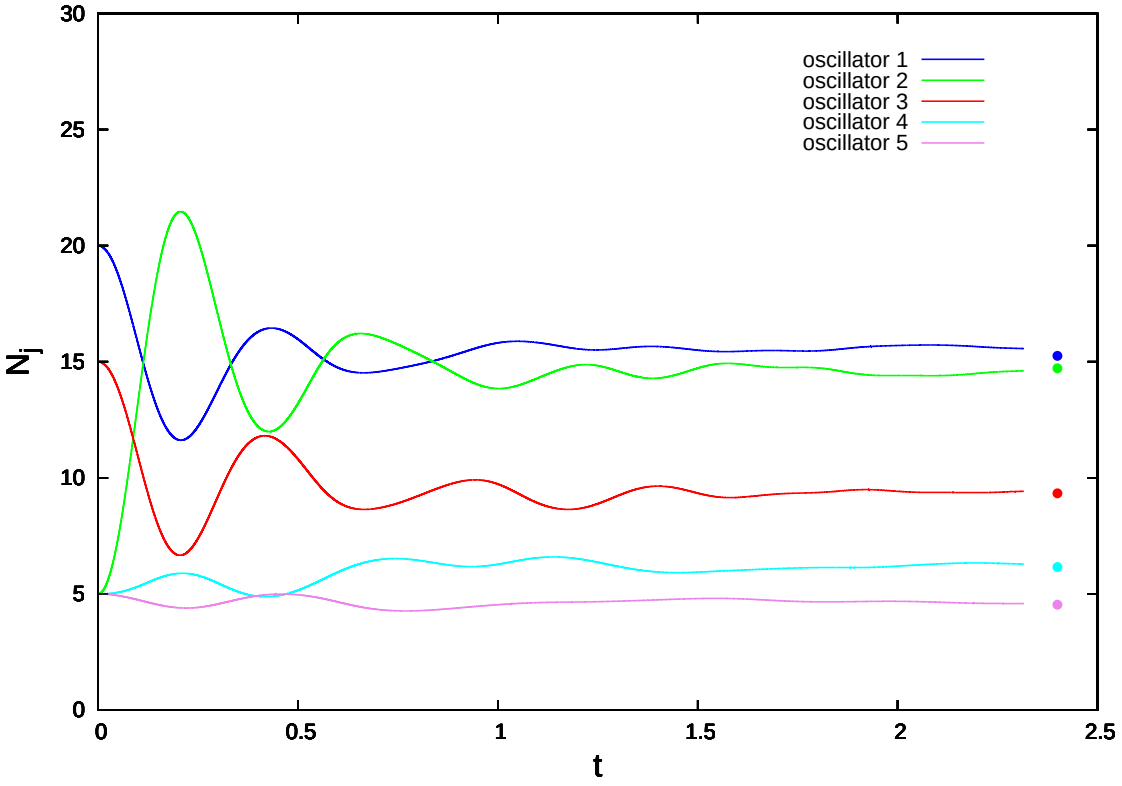

FIG. 1: Time evolution of the quantum mechanical average particle number $< \mathcal{N}_j >, j = 1..5$, in each of the five states of the toy model described in the text, starting with the initial state $(\mathcal{N}_1, ...\mathcal{N}_5) = (20,\ 5,\ 15,\ 5,\ 5)$. The dots indicate the thermal averages $\bar{\mathcal{N}}_j$ for the corresponding total energy. The system reaches thermal equilibrium on a time scale $1/\Gamma \sim 0.6$.